

Ionization and Conformational Equilibria of Citric Acid: Delocalized Proton Binding in Solution

Sergio Madurga, Miroslava Nedyalkova, Francesc Mas, and Josep L. Garcés

J. Phys. Chem. A, **Just Accepted Manuscript** • DOI: 10.1021/acs.jpca.7b05089 • Publication Date (Web): 13 Jul 2017

Downloaded from <http://pubs.acs.org> on July 18, 2017

Just Accepted

“Just Accepted” manuscripts have been peer-reviewed and accepted for publication. They are posted online prior to technical editing, formatting for publication and author proofing. The American Chemical Society provides “Just Accepted” as a free service to the research community to expedite the dissemination of scientific material as soon as possible after acceptance. “Just Accepted” manuscripts appear in full in PDF format accompanied by an HTML abstract. “Just Accepted” manuscripts have been fully peer reviewed, but should not be considered the official version of record. They are accessible to all readers and citable by the Digital Object Identifier (DOI®). “Just Accepted” is an optional service offered to authors. Therefore, the “Just Accepted” Web site may not include all articles that will be published in the journal. After a manuscript is technically edited and formatted, it will be removed from the “Just Accepted” Web site and published as an ASAP article. Note that technical editing may introduce minor changes to the manuscript text and/or graphics which could affect content, and all legal disclaimers and ethical guidelines that apply to the journal pertain. ACS cannot be held responsible for errors or consequences arising from the use of information contained in these “Just Accepted” manuscripts.

Ionization and Conformational Equilibria of Citric Acid: Delocalized Proton Binding in Solution

Sergio Madurga,^{*,†} Miroslava Nedyalkova,[‡] Francesc Mas,[†] and Josep Lluís Garcés[¶]

[†]*Materials Science and Physical Chemistry Department & Research Institute of Theoretical and Computational Chemistry (IQTCUB) of Barcelona University (UB), C/ Martí i Franquès, 1. 08028 Barcelona (Catalonia, Spain)*

[‡]*Inorganic Chemistry Department, Faculty of Chemistry and Pharmacy “St Kliment Ohridski”, University of Sofia, 1 James Bourchier Blvd. 1164, Sofia (Bulgaria)*

[¶]*Chemistry Department and AGROTECNIO, University of Lleida (UdL), Rovira Roure, 191, 25198, Lleida (Catalonia, Spain)*

E-mail: s.madurga@ub.edu

Abstract

The micro-speciation of citric acid is studied by analyzing NMR titration data. When the site binding (SB) model, which assumes fully localized proton binding to the carboxylic groups, is used to obtain microscopic energy parameters (dissociation constants, pair and triplet interaction energies between charged carboxylate groups), contradictory results are obtained. The resulting macroscopic constants are in very good agreement with the values reported in the literature using potentiometry. However, the found pair interaction energy between the terminal carboxylates and the triplet interaction energy are physically meaningless. In order to solve this apparent contradiction we consider the possibility of delocalized

1
2
3
4 proton binding, so that the proton can be exchanged at high velocity in the NMR time scale
5 through short, strong, low-barrier (SSLB) hydrogen bonds. With this aim, *ab initio* MP2 cal-
6 culations using the SMD polarizable continuum model for the solvent were performed and
7 the fully roto-microspeciation elucidated. Firstly, fully localized proton binding was assumed,
8 and the resulting micro-state probabilities are in reasonable agreement with those reported
9 in previous works which use selective blocking of the carboxylic groups. They are, how-
10 ever, in clear disagreement with the microstate probabilities derived from the NMR titration
11 data, which predict, within a very narrow confidence interval, a unique micro-species for the
12 symmetric di-ionized form. Moreover, counterintuitively, the interaction between terminal
13 charged groups is much larger than that between central and terminal groups. As a con-
14 sequence, we have explored the possibility of delocalized proton binding by calculating the
15 energy of intermediate proton positions between two carboxylic groups. The results reveal
16 that the exchange of the proton through the hydrogen bonds is in some cases produced with-
17 out energetic barrier. This effect is specially relevant in the di-ionized form, with all the most
18 stable conformations forming a SSLB, which together would constitute the only micro-state
19 detected by NMR. An alternative reaction scheme for the ionization process, based on proton
20 delocalization, is proposed.
21
22
23
24
25
26
27
28
29
30
31
32
33
34
35
36
37

38 Introduction

39
40
41 Citric acid is an important molecule involved in a broad range of biological, industrial and en-
42 vironmental processes.¹ For instance, it is a natural preservative and flavoring agent used in the
43 food industry² or a removable agent for heavy metal ions from waste-water.³ Citrate is also rel-
44 evant in colloidal sciences, where it is used as a common stabilizer and a reducing agent in the
45 synthesis of gold nanoparticles, or as a coating on nanomaterials for biological applications.⁴
46 It is also involved in differential adsorption on crystal surfaces leading to differential growing
47 of crystal geometries.⁵ All these properties are pH-dependent, so that a detailed knowledge of
48 the ionization mechanism of this small molecule is necessary. However, most of the studies on
49
50
51
52
53
54
55
56
57
58
59
60

1
2
3 the ionization properties of citric acid have been approached within the macroscopic picture.
4
5 Each protonation step is described by an equilibrium reaction characterized by a macroscopic
6
7 equilibrium constant. Citric acid have three ionizable carboxylic groups, and the correspond-
8
9 ing macroscopic dissociation constants have been mostly measured using potentiometry, in a
10
11 wide range of ionic strengths and temperatures, in presence of different ground electrolytes.⁶⁻⁹
12
13 However, in the macroscopic approach, no information is provided about the population of the
14
15 micro-states, for which the protonation state of every individual site is specified.¹⁰⁻¹² In the case
16
17 of citric acid, there is still controversy about the micro-state populations compatible with the
18
19 macroscopic dissociation constants.¹³⁻¹⁵
20

21
22 Micro-speciation of ionizable molecules, and in particular that of citric acid, has mainly been
23
24 performed within the context of the site-binding (SB) model, for which every protonating site can
25
26 adopt two possible states, *i.e.*, protonated or deprotonated. This means that the proton is localized
27
28 and ascribed to a unique protonating group, *i.e.*, it can not be shared by two ionizable sites. The
29
30 SB model has been successfully used in a wide range of molecules, ranging from small molecules
31
32 to polyelectrolytes and proteins, both for proton and metal binding.^{11,16,17} Within this framework,
33
34 two approaches have been applied to the determination of the molecular micro-speciation. In the
35
36 so-called 'deductive' methods, the molecule is modified so that one or several ionizable groups
37
38 are blocked. The non-blocked groups are supposed to have the same ionization properties as
39
40 in the original molecule. This assumption is the weakest part of the approach since changes in
41
42 the chemical structure of the molecule could modify the conformational and thus the chemical
43
44 environment of the rest of the groups,^{12,18} including the possible alteration or even destruction of
45
46 hydrogen bonds. In the case of citric acid, several authors have selectively blocked the carboxylic
47
48 groups forming the corresponding methyl-esters. The reported results, although consistent with
49
50 the value of the macroscopic constants, differ in the micro-state populations.¹³⁻¹⁵
51

52
53 A second approach applied to the determination of the micro-speciation of small molecules
54
55 is the use of spectroscopic techniques which are sensitive to the protonation of specific sites
56
57 and do not perturb the conformational structure of the molecule. Among them, high resolution
58
59
60

1
2
3
4 NMR is probably the most versatile and has been widely used in the micro-speciation of a vast
5 array of ionizable molecules ranging from proteins to small molecules.^{10–12,19–22} The chemical
6 shift of a nucleus located in the proximity of an ionizable group is sensitive to its protonation
7 state. Actually, it has been shown that, if the conformational equilibria are fast enough, the
8 chemical shift is a linear combination of the degree of protonation of the neighbouring sites.^{10,23}
9
10 As a consequence, measures of the chemical shift vs pH provide information about the micro-
11 speciation of the molecule. Citric acid is an AB spin system with two sets of coupled methylene
12 protons (Fig. 1). Moore and Sillerud measured the pH dependence of the high resolution NMR
13 spectra of citric acid, including both the chemical shift and the spin-spin coupling,²⁴ although no
14 micro-speciation analysis was reported.

15
16
17
18
19
20
21
22
23
24 However, situations have been reported for which the proton can be hardly ascribed to an in-
25 dividual donor group, the so called short, strong, low-barrier hydrogen bonds (SSLB-HB). SSLB-
26 HB present a very low energetic barrier between the asymmetric forms $A - O - H \cdots O - B$
27 and $A - O \cdots H - O - B$, so that the location of the proton should be regarded as indetermi-
28 nate. The resulting resonance structure $A - O \cdots H \cdots O - B$ seems to show extra strength or
29 stability, and has attracted great interest in the last years because of their possible role in the sta-
30 bilization of transition states in enzymatic reactions.²⁵ The existence of SSLB-HB has been widely
31 accepted in solid state. For instance, neutron diffraction analysis of the crystals of monoanions of
32 dicarboxylic acids, such as maleate or phthalate, show that the proton is centered between the two
33 donor oxygens.^{26–28} The same conclusion has also been achieved in X-ray crystal analysis, where
34 the separations between the two donor oxygen atoms are characteristically short, compared to
35 the usual, asymmetric, hydrogen bonds.^{29,30} In solution, however, the matter is more controver-
36 sial. The study of UV and IR spectra of poly(fumaric) and poly(maleic) acids by Kawaguchi *et*
37 *al.* suggests the existence of shared protons between consecutive carboxylic groups, forming a
38 kind of third species besides the “fully” protonated and “fully” deprotonated groups.³¹ Recent
39 research has shown the existence of dicoordinated proton in condensed media. An archetypal
40 example would be the bisdiethyletherate salts, composed by $H(OEt_2)_2^+$ cations and weakly coor-
41
42
43
44
45
46
47
48
49
50
51
52
53
54
55
56
57
58
59
60

1
2
3
4
5
6
7
8
9
10
11
12
13
14
15
16
17
18
19
20
21
22
23
24
25
26
27
28
29
30
31
32
33
34
35
36
37
38
39
40
41
42
43
44
45
46
47
48
49
50
51
52
53
54
55
56
57
58
59
60

dinating anions, being formed when strong acids are dissolved in diethyl ether.³² IR spectroscopy has shown that protons in liquid water form dicoordinated or even more complex structures of the kind of $[\text{H}(\text{H}_2\text{O})_n]^+$. Conversely, studies based on the NMR method of isotopic perturbation report that some of the dicoordinated structures existent in solid state, such as maleate, phthalate, among others, are, in solution, two tautomers in equilibrium differing in the solvation structure (or solvatomers) of the carboxylic groups, rather than a single symmetric species. However, even in this case, the H-bond of the solvatomers is not necessarily described by a double-well potential, but with a single-well potential with an additional contribution because of the instantaneous solvation.^{28,33} Thus, certain degree of bond asymmetry seems to be compatible up to some extent with proton delocalization. QM/MM calculations with explicit solvent have also shown the existence of a very low energetic barrier in the H-bond of the hydrogen-phthalate anion.³⁴

Regarding citric acid, previous *ab initio* calculations were performed to study its conformational properties without the consideration of delocalized hydrogen bonds. Khan *et al.*³⁵ generated conformations of citric acid and its dissociated forms using a Monte Carlo method with a classical force-field. The low energy conformers were optimized with the B3LYP/6-31+G level in the gas phase and the polarized continuum model was used to perform single point solvent calculations. Wrigth *et al.*³⁶ performed Carr-Parrinello molecular dynamics simulations for the completely deprotonated form of citric acid to obtain force-field parameters.

In the present work, we consider the possibility of delocalized proton in some of the ionization micro-states of citric acid by means of NMR titration data analysis, on the one side, and *ab initio* calculations using the SMD polarizable continuum model for the solvent,³⁷ on the other. A brief summary of both methodologies is provided in section 2. The available NMR titration data reported by Moore and Sillerud in ref.²⁴ are analyzed in section 3 within the SB model, *i.e.*, a bound proton is ascribed to a unique carboxylic group. Microscopic ionization constants, interactions between ionized groups and micro-state probabilities are obtained. The robustness of the best fitted parameters is tested by using Monte Carlo simulations of synthetic data sets. The results, however, seem to be in part inconsistent with fully localized proton binding. Some of the obtained

1
2
3 interaction energies, within a very narrow confidence interval, show nonphysical values, despite
4 the macroscopic constants are in very good agreement with those previously obtained by using
5 potentiometric titration under similar conditions. In particular, counterintuitively, the interaction
6 between terminal charged groups is much larger than that between central and terminal groups.
7 This fact could be explained because the reaction scheme does not take into account the possibil-
8 ity of delocalized proton binding in some roto-microstates, so that artificial effective interaction
9 energies are found. This possibility is discussed in section 4, where the *ab initio* calculations are
10 presented. With this aim, we perform an exhaustive scan of the most probable conformational
11 states within a particular macrostate (or roto-microstates), with special regard to those involving
12 H-bonds. The computations suggest that delocalized proton binding could be taking place in the
13 mono-ionized and di-ionized roto-microstates, with the proton moving without energetic barrier
14 between the ionized carboxylic group. This phenomenon could explain the anomalies detected
15 in the NMR analysis.
16
17
18
19
20
21
22
23
24
25
26
27
28
29
30
31

32 Methodologies

33 Macrostates, Microstates and Roto-microstates. Site Binding (SB) model

34
35
36 Let us firstly assume fully localized proton binding, so that a bound proton is ascribed to a unique
37 ionizable group. This is the starting hypothesis of the so-called site binding (SB) model. A par-
38 ticular conformational and ionization state, or *roto-microstate*, of a molecule with n protonated
39 sites is fully characterized by the probability $p_n(c, q, a_H)$, where a_H denotes the proton activity,
40 q the ionization state and c a particular conformational state. The ionization state q is defined
41 by a set of variables $q = \{q_1, q_2, \dots, q_N\}$, where N is the total number of ionizable sites. q_i can
42 take two possible values: $q_i = 1$ is the site is charged (*i.e.* deprotonated) and $q_i = 0$ otherwise.
43
44
45
46
47
48
49
50
51
52
53 $n = N - \sum_{i=1, \dots, N} q_i$ is the total number of protonated groups and define a *macrostate* n .
54
55
56
57
58
59
60

It can be shown that $p_n(c, q, a_H)$ can be expressed in the form³⁸

$$p_n(c, q, a_H) = \rho_n(c, q) P_n(a_H) \quad (1)$$

$\rho_n(c, s)$ represents the conditional probability of a roto-microstate provided that belongs to a macrostate n . $P_n(a_H)$ is the macrostate probability and it is given by

$$P_n(a_H) = \frac{\bar{K}_n a_H^n}{\Xi} \quad (2)$$

where \bar{K}_n are the macroscopic protonation constants and $\Xi = \sum_{i=0, \dots, N} \bar{K}_i a_H^i$ (with $\bar{K}_0 = 1$) is the semi-grand canonical partition function. \bar{K}_n corresponds to the process of binding n protons to the fully deprotonated molecule. The set of \bar{K}_n characterizes the macroscopic description, which does not differentiate between individual protonated groups. Note that, according to eqn. (1) the pH-dependence of the roto-microstate probabilities comes only from the macrostates probabilities, while the conditional probabilities are pH independent.^{11,38} For carboxylic acids as citric acid, the experimental quantities currently reported are the dissociation pK_i -values. pK_i corresponds to the process of releasing the i th proton, i.e., the deprotonation of the species with $N-i+1$ protons. K_i and \bar{K}_n are related by $pK_i = -\log K_i = \log(\bar{K}_{N-i+1}/\bar{K}_{N-i})$. Finally, a microstate s is defined as the set of roto-microstates with the same ionization state.³⁸ The microstate probability is given by

$$\pi_n(q) = \sum_c \rho_n(c, q) \quad (3)$$

and represents the conditional probability of a microstate s within a macrostate n . The microstate probabilities are related to the microstate free energy as

$$\pi_n(q) = \frac{e^{-\beta F(q)}}{\sum_s e^{-\beta F(q)}} \quad (4)$$

which can be expressed in the form of the so-called cluster expansion

$$\frac{\beta F(q)}{\ln 10} = \sum_i p k_i q_i + \sum_{j>i} \epsilon_{ij} q_i q_j + \sum_{k>j>i} \lambda_{ijk} q_i q_j q_k + \dots \quad (5)$$

where $\beta = 1/k_B T$, $p k_i$ is the microscopic dissociation constant of the site i ; ϵ_{ij} is the pair interaction energy between the charged sites i and j ; λ_{ijk} represents the triplet interaction energy, etc. $p k_i$, ϵ_{ij} , λ_{ijk} , the cluster parameters, do not depend on the conformational state, and they are proper averages of the roto-microstates.^{38,39} Note that the choice of the protonation variables is not unique. For instance, for polycations such as polyamines, a better choice is the set of variables $s_i = 1 - q_i$, so that the interaction terms are non zero when the sites are charged, *i.e.* protonated. For polyanions, however, the choice of the variables q_i seems more natural since the carboxylic groups are charged when they are deprotonated. In any case, the choice of the protonation variables does not affect the resulting thermal averages.¹¹ For citric acid, eqn. 5 can be simplified using the symmetry of the molecule. Since the two terminal carboxylic groups are equivalent, the cluster expansion remains

$$\frac{\beta F(q)}{\ln 10} = p k_1 (q_1 + q_3) + p k_2 q_2 + \epsilon_{12} (q_1 q_2 + q_2 q_3) + \epsilon_{13} q_1 q_3 + \lambda_{123} q_1 q_2 q_3 \quad (6)$$

so that five parameters are necessary to fully characterize the micro-speciation of citric acid, as depicted in Fig. 2a. They can be experimentally obtained by the techniques outlined in the introduction. In this work the pH dependence of the NMR chemical shifts of citric acid is analyzed.

NMR titrations and SB model

If the conformational and protonation equilibria are fast enough, it can be rigorously shown that the chemical shift of a particular atom α close to a ionizable group is given by the average of the chemical shifts of the possible roto-microstates of the molecule.⁴⁰ The simple form of the NMR spectrum of citric acid, shown in Fig. 1 indicates that this hypothesis is fulfilled by citric acid.²⁴

The chemical shift of a ^1H nucleus close to an ionizable group at a given pH, $\delta_\alpha(a_{\text{H}})$, is then given by¹²

$$\delta_\alpha(a_{\text{H}}) = \sum_{c,q} \delta'_\alpha(c,q) p_n(c,q,a_{\text{H}}) \quad (7)$$

where $\delta'_\alpha(c,q)$ is the chemical shift corresponding to the atom α when the molecule is in a particular roto-microstate (c,q) . Eqn. (7) together with (1) leads to

$$\delta_\alpha(a_{\text{H}}) = \sum_{n=0,\dots,N} \tilde{\delta}_{\alpha n} P_n(a_{\text{H}}) \quad (8)$$

where $\tilde{\delta}_{\alpha n} = \sum_{c,s} \delta'_\alpha(c,q) \rho_n(c,q) \delta_{n,\sum_{i=1,\dots,N} s_i}$, $s_i = 1 - q_i$ and $\delta_{n,\sum_{i=1,\dots,N} s_i}$ is the Kronecker delta, which takes the value 1 when there are exactly n protons, and 0 otherwise. Note that $\tilde{\delta}_{\alpha n}$ corresponds to the average of the chemical shifts of the roto-microstates corresponding to the same macrostate. Eqn. (8), together with (2), allows determining the macroscopic constants by fitting the experimental chemical shifts as a function of the pH. This information can be also available by potentiometric titration. However, in order to obtain microscopic information, it is necessary to express $\delta_\alpha(a_{\text{H}})$ as a function of the site-specific degrees of protonation, $\theta_i(a_{\text{H}})$, $i = 1, \dots, N$. They are related to the macroscopic probabilities by

$$\theta_i(a_{\text{H}}) = \sum_{n=1,\dots,N} A_{in} P_n(a_{\text{H}}) \quad (9)$$

where the coefficients A_{in} are given by¹⁰

$$A_{in} = \sum_s s_i \pi_n(q) \delta_{n,\sum_{i=1,\dots,N} s_i} \quad (10)$$

Expressing the macroscopic probabilities in terms of $\theta_i(a_{\text{H}})$ by inverting equation (9), and using the fact that $P_0(a_{\text{H}}) = 1 - \sum_{n=1,\dots,N} P_n(a_{\text{H}})$, the chemical shift can be expressed in terms of

the site-specific degrees of protonation as the linear combination

$$\delta_{\alpha}(a_{\text{H}}) = \delta_{\alpha 0} + \sum_{i=1, \dots, N} \delta_{\alpha i} \theta_i(a_{\text{H}}) \quad (11)$$

where $\delta_{\alpha 0} = \tilde{\delta}_{\alpha 0}$ and $\delta_{\alpha i} = \sum_{n=1, \dots, N} (\mathbf{A}^{-1})_{ni} (\tilde{\delta}_{\alpha n} - \tilde{\delta}_{\alpha 0})$ can be regarded as the chemical shifts of each protonated site. A significant advantage in using eqn. (11) instead of (8) is that the symmetry properties of the molecule can be incorporated in the fitting process by assuming equal $\theta_i(a_{\text{H}})$ values for equivalent ionizable sites, as it is the case of the first and third carboxylic groups of citric acid. If chemical shift data *versus* pH are available for one or more reporter nucleus α , $\delta_{\alpha 0}$ and the cluster parameters can be experimentally obtained using eqns. (9-11) together with the symmetry properties of the molecule.

***Ab initio* calculations**

In this work, both roto-microstate and microstate probabilities are evaluated by *ab initio* calculations. The fully protonated form of the citric acid was first prepared in the extended conformation (Fig. 1a). The methylene carbons of the chain are denoted as C_1 , C_2 and C_3 , each of them bound to a carboxylic group, denoted as C_{t1}, C_{t3} (terminal carboxylic groups) and C_{c2} (central carboxylic group). In addition, C_2 is also bound to a hydroxyl group. These three carbons form the skeleton of the molecule. The rotational state of $C_1 - C_2$ and $C_2 - C_3$ bonds, referred to as “central bonds”, are characterized by two dihedral angles, ϕ_1 and ϕ_2 . The rotation of each central bond results in three possible minima: *trans* (or, for abbreviation *t*, with $\phi_i \simeq 0$); *gauche*⁺ (g^+ with $\phi_i \simeq 120$); and *gauche*⁻ (g^- with $\phi_i \simeq -120$). The central bonds are considered to be in the *trans* state when the molecule is fully extended. We have chosen Flory criteria to assign the sign of the rotations, according to which the state g^+ of ϕ_i is obtained by rotating the pendant groups of the carbon C_i in the counterclockwise direction⁴¹ (or, in an equivalent way, rotating the pendant groups of the carbon C_{i+1} in the clockwise direction). The possible conformational states of the central bonds are represented in Fig. 1b. For each rotational state of the central bonds, there are

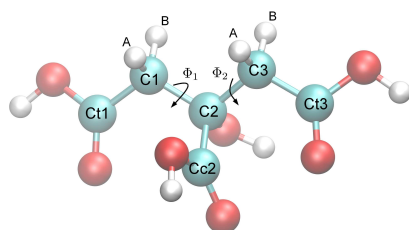
1
2
3 various possible dispositions of the carboxylic groups, which have also been explored. Because
4 of their important contribution to the conformational stability, special attention has been paid
5 for the viability of establishing intramolecular hydroxyl-carboxyl and carboxyl-carboxyl hydro-
6 gen bonds. With these criteria at hand, conformations were generated in a systematic way. The
7 geometry of the conformers was optimized at MP2 level with 6-311++G(d,p) basis set using the
8 SMD water model. All the *ab initio* calculations were carried out with Gaussian 09.⁴² Previous
9 studies⁴³⁻⁴⁵ have shown the accuracy and performance of the SMD implicit model for calculations
10 of solvation free energies. Frequency calculations in solution were performed for all the struc-
11 tures to confirm the absence of imaginary vibrational modes. The calculation of the vibrational
12 contribution to the free energy in solution is required for cases where liquid and gas-phase struc-
13 tures differ appreciably or when stationary points present in solution do not exist in gas phase.⁴⁶
14 Free energies and roto-microstate probabilities were obtained by performing statistical thermo-
15 dynamics calculations at 25°C, the temperature at which Moore *et al.* NMR experiments were
16 performed. Microstate probabilities were calculated using eqns. (3) and (4). The same approach
17 has been used for the rest of macrostates: the mono-ionized, di-ionized and fully ionized forms.
18
19
20
21
22
23
24
25
26
27
28
29
30
31
32
33
34
35

36 NMR titration of citric acid

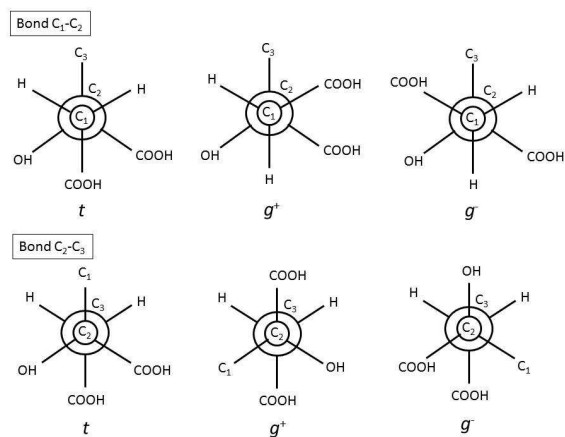
37
38 Citric acid has two non-equivalent methylene protons ($\alpha = A, B$) corresponding to the two peaks
39 of the NMR spectrum (Fig. 3). Both the separation of the peaks $\Delta = \delta_A - \delta_B$ and the average
40 position $\delta = (\delta_A + \delta_B) / 2$ are pH-dependent. Moreover, the two peaks are split by an amount
41 J , due to spin-spin coupling between the two hydrogen atoms. The pH-dependence of δ , Δ and
42 J is shown in Fig. 4. High resolution δ , Δ and J versus pH data were obtained by Moore and
43 Sillerud work.²⁴ The measurements were performed at 400 MHz and TMS was used as chemical
44 shift reference. For citric acid ($N = 3$), δ can be expressed by means of eqn. (11) as
45
46
47
48
49
50
51
52
53
54

$$55 \delta = \delta_0 + \delta_{13}\theta_1(a_H) + \delta_2\theta_2(a_H) \quad (12)$$

56
57
58
59
60



a)



b)

Figure 1: a) Representation of the fully extended citric acid molecule, showing the two main dihedral angles responsible for the conformational variability. Carbon atoms are depicted in blue, oxygen atoms in red and hydrogen atoms in white. The numbering of the carboxylic groups and the hydrogens (A and B) resolved in NMR experiments are also indicated. b) Representation of the three conformational minima obtained from the rotation of the $C_1 - C_2$ and $C_2 - C_3$ central bonds. The central bonds are considered to be in the *trans* (t) state when the molecule is fully extended. We have chosen Flory criteria to assign the sign of the rotations, according to this the state *gauge+* (g^+) of ϕ_i is obtained by rotating the pendant groups of the carbon C_i in the counterclockwise direction

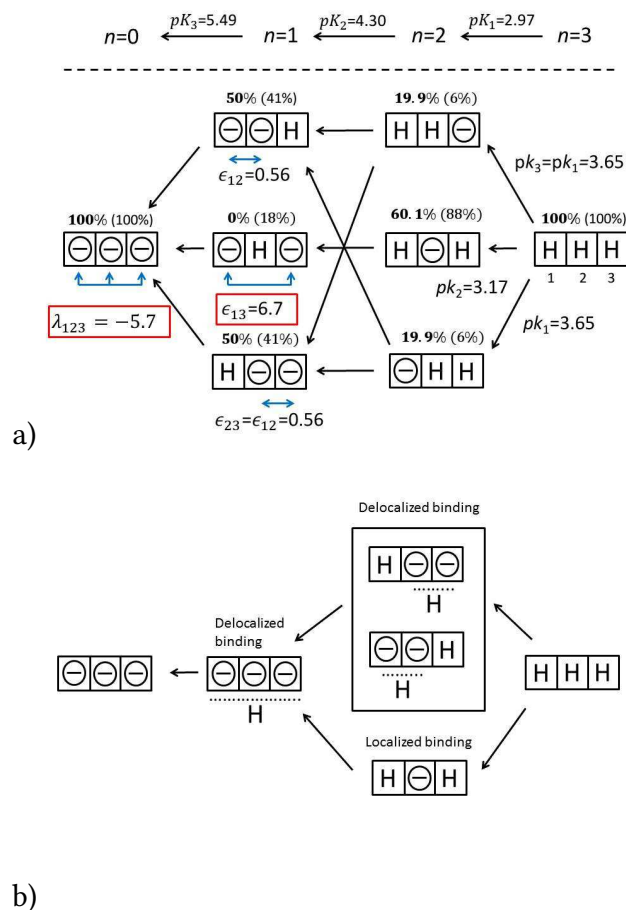


Figure 2: a) Reaction scheme of citric acid assuming fully localized proton binding. K_i are the macroscopic dissociation constants, calculated using the cluster parameters via eqns. 19. The fitted cluster parameters are reported: k_1 and k_2 are the dissociation microscopic constants of the terminal and central carboxylic groups, respectively. ϵ_{12} and ϵ_{13} represent the interaction energies between terminal-central and terminal-terminal dissociated carboxylic groups. Finally, λ_{123} accounts for the triplet interaction between the three dissociated carboxylic groups. The resulting microscopic probabilities are also shown (bold letters), and compared with *ab initio* calculations (between brackets). b) Reaction scheme considering the possibility of delocalized bindings. The roto-microspecies resulting from *ab initio* calculations are now classified into two groups: the ones which present delocalized proton binding and the ones which do not. Note that in the di-ionized form the proton can be exchanged among the three carboxylic groups, so that one micro-species is detected in the NMR time scale. In the mono-ionized form, however, both micro-states presenting localized and delocalized proton binding are possible.

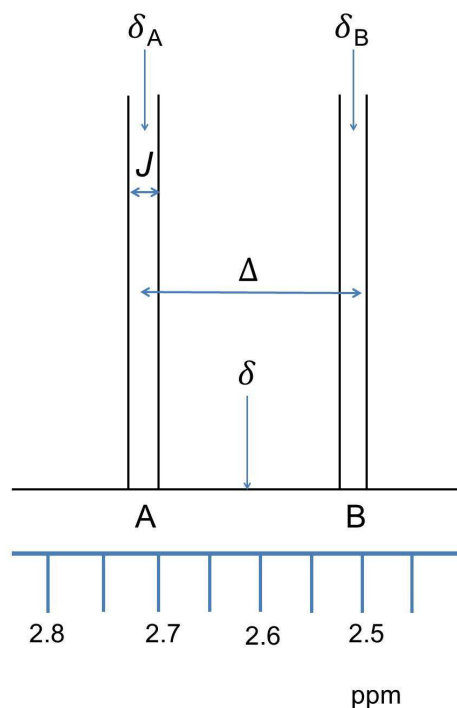


Figure 3: Sketch of the NMR citric acid spectrum corresponding to the two sets of non-equivalent methylene hydrogen atoms, A and B. The two peaks show spin-spin AB coupling, characterized by a coupling constant J . The position of the two peaks and the spin-spin coupling constant J are pH dependent. As a consequence, the average position of the two peaks ($\delta = (\delta_A + \delta_B) / 2$) and the separation between the two peaks ($\Delta = \delta_A - \delta_B$), reported by Moore and Sillerud²⁴ are also pH dependent. The assignment of each peak to a particular hydrogen atom, A or B, is only illustrative.

where $\delta_i \equiv (\delta_{Ai} + \delta_{Bi})/2$, ($i = 0, 1, 2, 3$). The symmetry property $\theta_1 = \theta_3$ has been used in (11) since the terminal carboxylic groups are equivalent. $\delta_{13} = \delta_1 + \delta_3$, and it accounts for the influence of both terminal carboxylic groups in the chemical shift. δ_0 , the average chemical shift for the fully deprotonated molecule, does not need to be fitted, since it can be obtained from the plateau of the experimental δ versus pH data in the region of high pH values, where the molecule is fully deprotonated (Fig. 4a). Moreover, δ_0 , δ_{13} and δ_2 are not independent, since at low enough pH values, the molecule is fully protonated ($\theta_i(a_H \rightarrow \infty) = 1$) giving the relationship $\delta_0 + \delta_{13} + \delta_2 = \delta_P$, where δ_P is the average chemical shift for the fully protonated molecule. The value of δ_P is obtained from the plateau of the δ versus pH data at low pH values. Then δ (from eqn.12) reads

$$\delta = \delta_0 + \delta_{13}\theta_1 + (\delta_P - \delta_0 - \delta_{13})\theta_2 \quad (13)$$

where δ_{13} is the only shift parameter to be fitted. In the same way, Δ can be expressed as

$$\Delta = \Delta_0 + \Delta_{13}\theta_1 + (\Delta_P - \Delta_0 - \Delta_{13})\theta_2 \quad (14)$$

and

$$J = J_0 + J_{13}\theta_1 + (J_P - J_0 - J_{13})\theta_2 \quad (15)$$

The validity of Eqns. (13-15) relies in the fact that δ , Δ and J are linear combinations of the chemical shifts of the four individual peaks, all of them fulfilling (11). The pH-dependence of δ , Δ and J comes from θ_1 and θ_2 . δ_0 , Δ_0 and J_0 are obtained from the plateau of the Figs. 4a, 4b and 4c at high enough pH values (2.42 ppm, 56.8 Hz and 15.22 Hz, respectively), while δ_P , Δ_P and J_P are obtained from the plateau at low pH values (2.81 ppm, 74.5 Hz and 15.86 Hz, respectively). δ_{13} , Δ_{13} and J_{13} are adjustable parameters. The chemical shifts corresponding to the individual peaks A and B, δ_A and δ_B are related with δ and Δ by

$$\delta_A = \delta - \frac{\Delta}{2f}; \quad \delta_B = \delta + \frac{\Delta}{2f} \quad (16)$$

where f is the spectrometer frequency. We preferred, however, to fit the original data δ , Δ and J rather than δ_A , δ_B and J since the peculiar shape of the curve Δ versus pH can show in a clearer way the quality of the fitting.

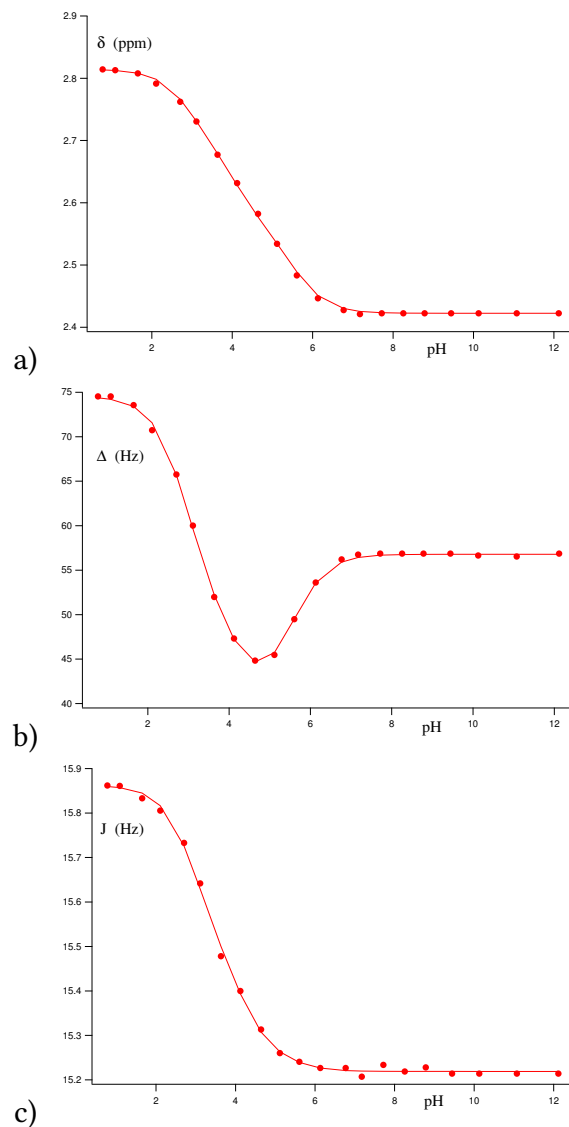


Figure 4: Markers: experimental average chemical shift (δ), separation between the center of the peaks (Δ) and spin-spin coupling (J) versus pH, taken from ref.²⁴ Continuous lines: best fitted curve obtained from eqns. (13-15) together with eqns. (18-20)

On the other hand, using (9-10), θ_1 and θ_2 can be expressed in terms of the macroscopic probabilities as

$$\begin{cases} \theta_1(a_H) = \pi_1(\text{H}\Theta\Theta) P_1(a_H) + (\pi_2(\text{H}\Theta\text{H}) + \pi_2(\text{HH}\Theta)) P_2(a_H) + P_3(a_H) \\ \theta_2(a_H) = \pi_1(\Theta\text{H}\Theta) P_1(a_H) + (\pi_2(\text{HH}\Theta) + \pi_2(\Theta\text{HH})) P_2(a_H) + P_3(a_H) \end{cases} \quad (17)$$

where H and Θ represent a protonated (-COOH) and a deprotonated (-COO⁻) site, respectively. The conditional probabilities are not independent since they are constrained by symmetry: $\pi_1(\Theta\Theta\text{H}) = \pi_1(\text{H}\Theta\Theta)$, $\pi_2(\Theta\text{HH}) = \pi_2(\text{HH}\Theta)$ and by the normalization conditions $\pi_1(\Theta\text{H}\Theta) + \pi_1(\text{H}\Theta\Theta) + \pi_1(\Theta\Theta\text{H}) = 1$ and $\pi_2(\text{H}\Theta\text{H}) + \pi_2(\text{HH}\Theta) + \pi_2(\Theta\text{HH}) = 1$. Therefore, there are only 2 independent conditional probabilities, for instance, $\pi_1(\text{H}\Theta\Theta)$ and $\pi_2(\text{HH}\Theta)$, and (17) can be rewritten as

$$\begin{cases} \theta_1(a_H) = \pi_1(\text{H}\Theta\Theta) P_1(a_H) + (1 - \pi_2(\text{HH}\Theta)) P_2(a_H) + P_3(a_H) \\ \theta_2(a_H) = (1 - 2\pi_1(\text{H}\Theta\Theta)) P_1(a_H) + 2\pi_2(\text{HH}\Theta) P_2(a_H) + P_3(a_H) \end{cases} \quad (18)$$

Eqns. (17) can be fully expressed in terms of the cluster parameters. The macrostate probabilities $P_i(a_H)$ depend on the macroconstants through eqns. 2, which, after some elementary calculations, can be related to the microscopic binding parameters of the cluster expansion (6) as follows

$$\begin{cases} K_1 = 2k_1 + k_2 \\ K_2 = \frac{k_1(2k_2u + k_1v)}{2k_1 + k_2} \\ K_3 = \frac{k_1k_2u^2vw}{2k_2u + k_1v} \end{cases} \quad (19)$$

with $\log u = -\epsilon_{12}$, $\log v = -\epsilon_{13}$ and $\log w = -\lambda_{123}$. The microstate probabilities are given by:

$$\pi_1(\text{H}\Theta\Theta) = \frac{k_2u}{2k_2u + k_1v}; \quad \pi_2(\text{HH}\Theta) = \frac{k_1}{2k_1 + k_2} \quad (20)$$

In summary, equations (13-15) and (18-20) contain eight parameters to be simultaneously fitted to the experimental chemical shifts: three chemical shift parameters (δ_{13} , Δ_{13} and J_{13}), two

1
2
3
4
5
6
7
8
9
10
11
12
13
14
15
16
17
18
19
20
21
22
23
24
25
26
27
28
29
30
31
32
33
34
35
36
37
38
39
40
41
42
43
44
45
46
47
48
49
50
51
52
53
54
55
56
57
58
59
60

microscopic dissociation constants (k_1 and k_2) and three interaction energies (ϵ_{12} , ϵ_{13} and λ_{123}). The fitting procedure has been performed using standard nonlinear regression routines of MATLAB.⁴⁷ The robustness of the fitting has been checked by means of Monte Carlo simulation of synthetic data, which provides accurate estimates of the parameter confidence intervals without requiring any assumption about the probability distribution of the parameters, or about the linearity of the fitted mathematical model.^{48,49} In this method, an initial best fitting is performed using the original data set. The average deviation between the best-fitted curve and the experimental data is taken as an estimation of the variance σ of the error probability distribution, which is assumed to be Gaussian. Then a new set of synthetic data set is generated by adding random errors to the experimental data. A fitting process is performed to the new data set and a new set of best-fitted parameters is obtained. The process is repeated a sufficiently large number of times (thousands in this work), and the resulting values for each particular fitted parameters are listed in numerical order. The confidence intervals of 95%, the ones reported in this work, are obtained by removing from the ordered list those values corresponding to the 0.5% of the upper and lower tail. Since the probability distribution of the parameters does not need to be Gaussian, the confidence intervals do not need be strictly symmetric. Hence both the upper and lower bounds of the limiting intervals are reported (see Tables 1 and 2). Confidence intervals for functions of the fitted parameters, such as microstate probabilities or macroscopic dissociation constants can be obtained by the same procedure.

The found NMR parameters in eqns. (12-15) are shown in Table 1. The best-fitted parameters δ_{13} , Δ_{13} and J_{13} are reported within 95% confidence intervals. If the fitting is performed only to δ and Δ data (Figs. 4a and 4b), without using the spin-spin coupling data (Fig. 4c) the results do not change significantly. This fact supports the consistency of the obtained values. δ , Δ and J for the fully protonated (δ_P , Δ_P and J_P) and the fully deprotonated (δ_0 , Δ_0 and J_0) molecule were not fitted but obtained from the plateaus of figs. 4 at low and high pH-values, respectively.

The cluster parameters are shown in Table 2, together with the ones calculated from the results reported in refs.^{14,15} These works make use of selective methyl substitution of the carboxylic

Table 1: Values of the δ_i , Δ_i and J_i NMR shift parameters for citric acid defined in eqns. 13-15. The NMR shifts corresponding to the fully deprotonated ($i=0$) or fully protonated ($i=P$) have been obtained from the plateau of the curves of Fig. 4 at high and low pH-values, respectively. δ_{13} , Δ_{13} and J_{13} have been fitted to the three experimental curves in Fig. 4 simultaneously. The 95% confidence interval has been estimated using a Monte Carlo method consisting in the generation of synthetic data with random Gaussian errors with variance 2σ . δ_2 , Δ_2 and J_2 have been calculated using $\delta_2 = \delta_P - \delta_0 - \delta_{13}$, $\Delta_2 = \Delta_P - \Delta_0 - \Delta_{13}$ and $J_2 = J_P - J_0 - J_{13}$, respectively.

i	13	0	P	2
δ_i (ppm)	0.28 (+0.02/-0.02)	2.42	2.81	0.11
J_i (Hz)	0.07 (+0.05/-0.06)	15.21	15.81	0.53
Δ_i (Hz)	-31.7 (+1.1/-1.2)	56.7	74.5	49.4

groups to deduce the complete ionization scheme of citric acid. The accuracy of these methods relies on the assumption that the non-blocked groups have the same ionization properties as the original molecule. Under this assumption, potentiometric titration of the modified molecules allows determining two of the cluster parameters (for instance pk_1 and ϵ_{12}). Provided that the macroscopic dissociation constants are known, the restant three cluster parameters can be obtained by solving the three eqns. 19. In the case of Martin work,¹⁴ we have used the macroscopic constants at $I=0.1$ M reported in Robertis *et al.*,⁵⁰ instead of those at infinite dilution,⁶ which leads to important discrepancies with Pearce *et al.* results.¹⁵ As previously pointed out in ref.,¹⁵ Martin does not state the concentrations of ester used in the titrations, but these are supposed to be high enough to significantly contribute to the ionic strength. This consideration seems confirmed by the good agreement between both works when the macroscopic dissociation constants are not taken at infinite dilution (Table 2).

The microscopic dissociation pk -values, $pk_1 = 3.65$, $pk_2 = 3.17$, and the nearest neighbour interaction energy, $\epsilon_{12} = 0.56$, are, within a narrow confidence interval, very similar to those obtained from refs.^{14,15} at 0.1M of KCl solution. However, the next-nearest interaction parameter ϵ_{13} and the triplet interaction parameter, λ_{123} clearly differ from those obtained from the previous works. The obtained values, $\epsilon_{13} = 6.68$ and $\lambda_{123} = -5.65$, represent enormous repulsive (9.1 kcal/mol) and attractive energies (-7.7 kcal/mol), respectively. Monte Carlo error analysis shows that this behaviour is very robust within the whole confidence intervals, reported in Table 2

1
2
3 indicate. In order to understand how unrealistic these values are, we can compare them with the
4 interaction energies of nearest-neighbour sites of other molecules whose ionizable groups are
5 separated by three bonds. For instance, for poly(maleic) and poly(fumaric) acids, with interactions
6 regarded as particularly strong, $\epsilon_{12} \simeq 1.5 - 3.9$, depending on the background electrolyte and
7 the bond tacticity; for succinic acid $\epsilon_{12} \simeq 0.8$;⁵¹ for poly(ethylene)imine, $\epsilon_{12} \simeq 2$ and $\lambda_{123} \simeq$
8 0.45 .⁵² Moreover, it is important to highlight the strange fact that the interaction energy between
9 terminal charged groups ϵ_{13} is much larger than that between a terminal and the central group.
10 This is counterintuitive and very difficult to justify in physical terms, since when the two terminal
11 groups are charged, the molecule can accommodate the conformation to get a larger distance
12 between the charged groups than when a terminal and a central group are charged.
13
14
15
16
17
18
19
20
21
22
23

24 Once the cluster parameters are determined, the macroscopic dissociation constants can be
25 calculated using eqns. 19. Interestingly, despite the unreliable values of ϵ_{13} and λ_{123} , the macro-
26 scopic constants, calculated using eqns. 19, are in good agreement with the values reported in
27 previous literature, as shown in Table 3. Especially remarkable is the agreement with the values
28 reported by Robertis *et al.*⁵⁰ (with $I=0.1\text{M}$ and $I=0.5\text{ M}$), Crea *et al.*⁸ (with $I=0.5\text{M}$), and Bénézech
29 *et al.*⁷ ($I=0.1\text{m}$ and $I=0.5\text{ m}$). They also agree with other experimental studies,^{9,53,54} and calcu-
30 lations using the Pitzer theory.^{8,50,55} In contrast, they differ with the values obtained at infinite
31 dilution.⁶ This discrepancy is expected since the NMR experiments were done at a sodium citrate
32 concentration 0.1 M , so that the minimum value of the ionic strength in the titration experiment
33 was $I=0.3\text{ M}$.
34
35
36
37
38
39
40
41
42
43

44 In summary, in analyzing the pH-dependence of the NMR chemical shifts by means of the
45 SB model, *i.e.*, assuming fully localized proton binding, we arrive to contradictory results: on the
46 one side, we obtain good values for the macroscopic constants, in agreement with those obtained
47 previously with potentiometry. But, on the other side, we get nonphysical values for the interac-
48 tion energies. This intriguing fact is also reflected in the obtained microstate probabilities, which
49 are shown in Table 4. They clearly differ from those obtained from refs.¹⁴ and.¹⁵ These works
50 predict a significant presence of the symmetric di-ionized microstate ($\ominus\text{H}\ominus$) (around 10-15%).
51
52
53
54
55
56
57
58
59
60

As will be shown in section 4, *ab initio* computations assuming localized proton binding also lead to the same conclusion. Conversely, our analysis shows that, within a very narrow confidence interval, this microstate is virtually nonexistent, so that only the asymmetric di-ionized microstate is present. Algebraic arguments, complementary to the Monte Carlo test, can also be used to justify the robustness of this result. The analysis, outlined in the supporting information, shows the existence of a unique minimum in the fitting process. The nonexistence of the di-ionized symmetric microstate is equivalent to a huge repulsive energy between the terminal carboxylates. In the same way, this huge repulsive energy must be compensated by an enormous triplet attractive energy to produce the tri-ionized state. Actually, it can be shown that the confidence interval for the sum of ϵ_{13} and λ_{123} is very narrow, so that triplet interactions always compensate the terminal-terminal carboxylate repulsion.

In this work we propose that this result, clearly an artifact, could be the consequence of trying to analyze the NMR shifts assuming fully localized proton. Aiming at clarifying this point, in the next section a systematic scan of the most stable conformations of citric acid is performed. As will be shown, some of these conformations allow proton exchange between carboxylic groups without energetic barrier, so that the basic assumption of the SB model, i.e., the assignment a carboxylic group to a bound proton, is no longer suitable to understand the ionization properties of citric acid. It is worth to note that proton delocalization can not take place in the experiments which use selective methylation of the carboxylic groups. This would explain the observed discrepancies with the results obtained from NMR titrations.

Table 2: Cluster parameters of citric acid at 25°C obtained by fitting the SB model (eqns. 18-19) to NMR titration data taken from ref.²⁴ The best-fitted values are given within 95% confidence intervals, which are reported between brackets. The values calculated from refs.¹⁴ and¹⁵ which use selective methylation of the carboxylic groups, are also reported.

	pk_1	pk_2	ϵ_{12}	ϵ_{13}	λ_{123}
fitted from NMR titration	3.65	3.17	0.56	6.68	-5.65
$I \geq 0.3$ M	(+0.04/ -0.03)	(+0.03/ -0.02)	(+0.08/ -0.08)	(+4.02/ -4.63)	(+4.67/ -4.07)
Martin ¹⁴ $I \sim 0.1$ M	3.85	3.35	0.73	0.54	-0.28
Pearce <i>et al.</i> ¹⁵ $I = 0.1$ M	3.79	3.02	0.78	0.62	-0.15

Table 3: Macroscopic pK -values of citric acid at 25°C calculated using the cluster parameters obtained from NMR titrations (Table 2) and eqns. (19), together with values previously reported in the literature, determined by potentiometry.

	pK_1	pK_2	pK_3
from NMR titrations (Table 2)	2.95	4.13	5.54
using eqns. 19, $I \geq 0.3$ M	(+0.03/-0.03)	(+0.05/-0.05)	(+0.05/-0.05)
Bates <i>et al.</i> ⁶ $I \sim 0$ M	3.13±0.02	4.76±0.01	6.40±0.01
Pearce <i>et al.</i> ¹⁵ $I \sim 0$ M	3.04	4.70	5.77
Robertis <i>et al.</i> ⁵⁰ $I=0.1$ M	2.92	4.35	5.77-5.78
Bénezeth <i>et al.</i> ⁷ $I=0.1$ m	2.90±0.01	4.34±0.01	5.68±0.02
Robertis <i>et al.</i> ⁵⁰ $I=0.5$ M	2.82	4.13-4.15	5.41-5.44
Crea <i>et al.</i> ⁸ $I=0.5$ M	2.81-2.82	4.11-4.15	5.31-5.44
Bénezeth <i>et al.</i> ⁷ $I=0.5$ m	2.77±0.01	4.12±0.02	5.27±0.04

Table 4: Microstate probabilities assuming fully localized proton binding at 25°C, calculated replacing the found cluster parameters (Table 2) in eqns. (20), together with values previously reported in the literature, determined by potentiometry.

	π_2 (H Θ H)	π_2 (HH Θ)= π_2 (Θ HH)	π_1 (Θ H Θ)	π_1 (H Θ Θ)= π_1 (Θ Θ H)
fitted from NMR titration	60.1%	19.9%	0.0%	50.0%
$I \geq 0.3$ M	(+0.5/ -0.0)	(+0.2/ -0.3)	(+0.4/ -0.0)	(+0.0/ -0.2)
<i>ab initio</i> calculations $I = 0$ M	88%	6%	18%	41%
Martin ¹⁴ $I \sim 0.1$ M	77%	11.5%	10.6%	44.7%
Pearce <i>et al.</i> ¹⁵ $I \sim 0$ M (exp)	79%	10.5%	11%	44.5%
Pearce <i>et al.</i> ¹⁵ $I = 0.1$ M (exp)	75%	12.5%	14%	43%

***Ab initio* calculations and hydrogen bond formation. Localized versus delocalized proton binding**

The most stable roto-microstates of citric acid for the different degrees of ionization are shown in Table 5. They are obtained by means of *ab initio* MP2 computations with 6-311++G(d,p) basis set using SMD water model. Free energies values are reported as relative to the most stable roto-microstate of the same macrostate, which is given zero free energy. The roto-microstate probability within a specific macrostate is then calculated using the Boltzmann distribution at the same temperature of NMR experiments, 25°C. The possibility of state multiplicity due to symmetry is also taken into account in the calculations. Only roto-microstates with probability larger than 0.9% are shown in Table 5. The rest of them are reported in the supplementary information. Once a particular macrostate was fixed, the conformational search of citric acid was carried out preparing initial structures with *gauche+*, *gauche-* and *trans* conformations for ϕ_1 and ϕ_2 dihedral angles. In addition, different orientations of the hydroxyl and carboxylic groups were also sampled in a systematic way. Special attention has been paid to the formation of carboxyl-carboxyl and carboxyl-hydroxyl hydrogen bonds because of their stabilizing capacity of the conformation. The HB bond distance is also shown in Table 5. We consider that a HB is formed if the distance between oxygen atoms is less than 3 angstroms and the angle O-H-O is larger than 120 degrees. HB bonds between two carboxylic groups, one of them acting as an acceptor and the other one as a donor, are indicated in the Table by an overbar on the corresponding deprotonated (“ \ominus ”) or protonated (“H”) site. The computations have firstly been performed assuming fully localized proton binding.

In Table 5, the roto-microstates are depicted by means of two letters indicating the conformations of ϕ_1 and ϕ_2 dihedral angles, followed by a number indicating the relative stability with respect to the most stable roto-microstate having the same conformation. There is also an additional sub-index expressing the ionization state (0, -1, -2, -3). So, for instance, tg^{+1}_{-2} represents a di-ionized roto-microstate with ϕ_1 in *trans* state, ϕ_2 in *gauche+* state, and with the most stable

1
2
3
4 disposition in the tg^+ conformation.

5
6 For the fully protonated molecule, $C_6H_8O_7$, three minima were found with significant pop-
7 ulation: one for tt and two for tg^+ . $tt1_0$ corresponds to the fully extended molecule being the
8 most stable one (88%). It is not completely symmetric ($\phi_1 \neq -\phi_2$), since the hydroxyl group
9 is oriented towards one of the terminal carboxylic groups while the other terminal carboxylic
10 group is oriented differently. Roto-microstates tg^+1_0 and tg^+2_0 , with very similar free energies,
11 are much less abundant (7.0% and 4.5%, respectively). In tg^+1_0 and tg^+2_0 the hydroxyl group
12 points towards the *gauche* and the *trans* part of the molecule, respectively.
13
14
15
16
17
18
19

20 In the case of the fully deprotonated citrate anion, $C_6H_5O_7^{-3}$, the most stable conformation
21 is $tt1_{-3}$ followed by tg^+1_{-3} (0.4 kcal/mol). Thus, $tt1_{-3}$ has the greatest abundant of the fully
22 deprotonated form, with 62 %, followed by 33% of abundance for tg^+1_{-3}
23
24
25

26 For the hydrogen citrate anion, $C_6H_7O_7^{-1}$, the more stable conformers are of the type tt (with
27 five dispositions), tg^+ (one disposition) and g^-g^- (five dispositions). The most stables structures,
28 depicted in Fig. 5a and 5b, correspond to $tt1_{-1}$ (with probability of 23%) and $g^-g^-1_{-1}$ (48%)
29 conformations, with the same free energy. Assuming fully localized binding, in both cases the
30 central carboxylic group is ionized. In the case of $g^-g^-1_{-1}$, a HB bond is formed between the
31 central deionized carboxyl and the terminal one, which clearly stabilizes this conformation. To-
32 gether with the roto-microstates $tt2_{-1}$, $tt3_{-1}$, $tt4_{-1}$, $tt5_{-1}$ and tg^+1_{-1} , all of them with an
33 ionized central carboxyl, the resulting probability for the symmetric charged form is 88%. This
34 is in agreement with refs.,^{14,15} where the micro-state probabilities were obtained using selective
35 methylation of the carboxylic groups, a technique for which HB are destroyed and therefore
36 delocalized proton binding is unavoidable. The comparison with the micro-state probabilities
37 obtained from these experiments is shown in Table 4. The agreement is remarkable taking into
38 account that water has been included implicitly. Models with implicit solvent have revealed to be
39 very useful in, for instance, differential solvation in chemical reactions.⁵⁶ More complete models
40 including explicit water could lead to a more complete picture and are object of current research.
41
42
43
44
45
46
47
48
49
50
51
52
53
54

55 For the di-ionized species, $C_6H_6O_7^{-2}$, again reasonable agreement between our *ab initio* calcu-
56
57
58
59
60

lations and refs.^{14,15} is obtained. However, the micro-state probabilities are in total contradiction with the NMR titration experiments. In our opinion, this discrepancy is, as revealed by Monte-Carlo statistical analysis, robust enough to inspect alternatives to the standard SB model.

The picture changes considerably if we accept the possibility that at least some of the formed HB allow the proton to be delocalized between two charged carboxylic groups. This means that, in reality, one should consider three possible states for the proton: localized in the central carboxyl, localized in the terminal carboxyl, and delocalized proton between two carboxylic groups. The existence of this 'third' species was proposed by Kawaguchi *et al.*,³¹ who suggested the existence of shared protons between consecutive carboxylic group to explain the pH-dependence of UV and IR spectra of poly(fumaric) and poly(maleic) acids. Let us firstly classify the roto-microstates of $C_6H_7O_7^{-1}$ into two groups: those which contain a HB bond between carboxylic groups and those which do not. $tt1_{-1}$ (with probability 23%), $tt5_{-1}$ (1.1%) and tg^+1_{-1} (6.1%), which all represent 30.2% of the roto-microstates, do not present any kind of HB. On the contrary, $g^-g^-1_{-1}$, $g^-g^-2_{-1}$, $tt2_{-1}$, $tt3_{-1}$ and $tt4_{-1}$ exhibit HB between the central and the terminal carboxylic groups. In the case of $tt2_{-1}$, moreover, the three carboxylic groups participate in hydrogen bonds, with the two terminal carboxylic groups acting as hydrogen donors and the central one as an acceptor. They are thus candidates to present proton delocalization.

Let's explore the possibility of proton delocalization by means of *ab initio* calculations. Firstly note that in the conformations $g^-g^-1_{-1}$ and $g^-g^-2_{-1}$, all the atoms have practically the same coordinates, except that of the acid hydrogen, as can be observed in Figs. 5b and 5c. A shift in the acid hydrogen position of about 0.3 angstroms makes to protonate a lateral ($g^-g^-1_{-1}$) or the central ($g^-g^-2_{-1}$) carboxylic group. In order to analyze the free energy profile of the transition, additional calculations were performed by locating the acid hydrogen atom at intermediate positions between both carboxylic groups. The obtained results are shown in Fig. 6a, where we have plotted energy *versus* distance to the center between the two oxygens. The resulting curve indicates that the transition between $g^-g^-1_{-1}$ and $g^-g^-2_{-1}$ is produced with a small energetic barrier of about 0.2 kcal/mol. The most stable conformer is obtained when the proton is

1
2
3 in between these two conformational minima. We can observe, however, that the localization of
4 the proton in this transformation is not symmetric, being more similar to the $g^-g^-1_{-1}$ minima.
5 There are also species without HB between carboxylic groups: $tt1_{-1}$, $tt5_{-1}$ and tg^+1_{-1} , all of
6 them corresponding to the symmetric form, for which the central carboxyl is ionized. Finally, in
7 the roto-microstates $tt2_{-1}$, $tt3_{-1}$ and $tt4_{-1}$ the central carboxylic group is ionized and the lateral
8 carboxyl groups are protonated, but in this case forming a HB without proton delocalization. It
9 is worth to note, that those HB that are localized are those with the greatest HB distances ($>$
10 1.48 \AA), while those that are delocalized (SSHB) have the shortest ones ($< 1.48 \text{ \AA}$) (Table 5). In
11 summary, the roto-microstates corresponding to the dihydrogen-citrate ion can be classified into
12 two groups: the symmetric form with localized terminal protons and the one with delocalized
13 protons. These values are very similar to the results obtained from NMR titrations, if the micro-
14 species are re-interpreted as symmetric with terminal localized protons *versus* asymmetric with
15 delocalized proton. The new interpretation of the reaction scheme is outlined in Fig. 2b. Unfor-
16 tunately, when proton delocalization taken into account, some information, such as the entropy
17 associated to proton delocalization, is lacking in order to rigorously estimate the probabilities of
18 localized and delocalized states.

19
20
21
22
23
24
25
26
27
28
29
30
31
32
33
34
35
36 In the case of the hydrogen-citrate anion $C_6H_6O_7^{-2}$, proton delocalization could play an even
37 more important role. All the most stable conformations reported in Table 5 can be transformed
38 one into other either by a conformational change, or by transference of delocalized a proton
39 through a HB without energetic barrier (SSLB). This means that at the NMR time scale, all the
40 roto-microstates behave on average as a unique microstate, which is consistent with the surpris-
41 ing 100% probability for only one microstate. A large part of the population (61%) is distributed
42 between only two minima: the $g^-g^-1_{-2}$ and $g^-g^-2_{-2}$ asymmetrical charged conformers (Figs.
43 5d and 5e). The only difference between these two conformers is the transference of a proton be-
44 tween the two terminal carboxyl groups. Calculations fixing the acid hydrogen at intermediate
45 positions indicates that this transition is performed without energetic barrier, as shown in Fig.
46 6b. Actually, the curve energy *versus* distance to the center of the oxygens is in this case very
47
48
49
50
51
52
53
54
55
56
57
58
59
60

1
2
3 symmetric and exhibits a minimum of about -2 kcal/mol. A similar situation is found for the pairs
4 of conformers $g^-g^-3_{-2}$ vs $g^-g^-4_{-2}$ and tg^+1_{-2} vs tg^+2_{-2} , as shown in Figs. 6c and 6d. Moreover,
5
6 $g^-g^-5_{-2}$ can be transformed into $g^-g^-4_{-2}$ and tg^+2_{-2} into tg^+3_{-2} just by a change in the dispo-
7
8 sition of the resting carboxylic group. As a consequence, within this new picture, there would not
9
10 be localized protons in the di-ionized form of citric acid, so that NMR can only detect a unique
11
12 species. We have depicted this result in Fig. 2b. The large discrepancy between the speciation re-
13
14 sulting from NMR titrations and previous works, based on methyl substitution emerges now as a
15
16 natural consequence of proton delocalization. Selected blocking of the carboxylic groups would
17
18 break the HB of the original molecule, so that the modified compound behaves as the original
19
20 one presenting only fully localized protons. This would also explain the rather good agreement,
21
22 within the limitations of the calculation technique, between “deductive” methods in refs.¹⁴ and¹⁵
23
24 and *ab initio* computations.
25
26
27

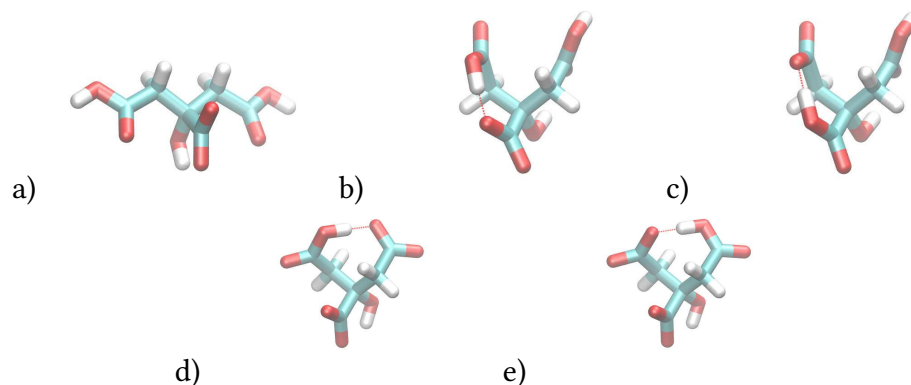


Figure 5: More stable roto-microstates of di-hydrogen citrate ($q=-1$): $tt1_{-1}$ ($H\Theta H$) (a), $g^-g^-1_{-1}$ ($H\Theta H$) (b) and $g^-g^-2_{-1}$ ($\Theta H\Theta$) (c); and hydrogen citrate ($q=-2$): $g^-g^-1_{-2}$ ($H\Theta\Theta$) (d) and $g^-g^-2_{-2}$ ($\Theta\Theta H$) (e). Oxygen atoms are depicted in red, carbons in green and hydrogen atoms in white.

53 54 55 56 57 58 59 60

The micro-speciation of citric acid is studied by analyzing NMR titration data. When fully localized proton binding is assumed, the so-called site-binding (SB) model, microscopic dissociation constants, together with pair and triplet interaction energies between charged carboxylate groups

Table 5: Relative free energies of conformations of citrate in water obtained by MP2 calculations for all the possible degrees of ionization (0,-1,-2,-3). “H” indicates a protonated carboxylic group while “ \ominus ” depicts a deprotonated carboxylic group. The participation of a carboxylic group in an intramolecular hydrogen bond between two carboxylic groups is indicated by an overbar over the corresponding “H” and “ \ominus ” sites. Only conformations with a proportion greater than 0.9% are shown. Relative Free energies in water (in kcal/mol) and hydrogen bond distances (in angstroms). Conformational proportions were calculated using proper Boltzmann factors at 25°C. The hydrogen bonds are classified into two groups: those which present localized proton binding and those who conform a SSLB-HB.

charge	conformation	protonation	ΔG_{rel} (kcal/mol)	Relative population	d(H...O) (Å)	HB type
0	<i>tt</i> 1 ₀	HHH	0.0	88%	–	–
	<i>tg</i> ⁺ 1 ₀	HHH	1.5	6.9%	–	–
	<i>tg</i> ⁺ 2 ₀	HHH	1.8	4.4%	–	–
-1	<i>tt</i> 1 ₋₁	H $\overline{\text{O}}$ H	0.0	23%	–	–
	<i>tt</i> 2 ₋₁	$\overline{\text{H}}$ $\overline{\text{O}}$ H	1.5	3.7%	1.50	local.
	<i>tt</i> 3 ₋₁	$\overline{\text{H}}$ $\overline{\text{O}}$ H	1.6	3.2%	1.63	local.
	<i>tt</i> 4 ₋₁	$\overline{\text{H}}$ $\overline{\text{O}}$ H	2.1	1.5%	2.13	local.
	<i>tt</i> 5 ₋₁	H $\overline{\text{O}}$ H	2.2	1.1%	–	–
	<i>tg</i> ⁺ 1 ₋₁	H $\overline{\text{O}}$ H	1.2	6.1%	–	–
	<i>g</i> ⁻ <i>g</i> ⁻ 1 ₋₁	$\overline{\text{H}}$ $\overline{\text{O}}$ H	0.0	48%	1.46	SSLB
<i>g</i> ⁻ <i>g</i> ⁻ 2 ₋₁	$\overline{\text{O}}$ HH	0.9	10%	1.36	SSLB	
-2	<i>tg</i> ⁺ 1 ₋₂	$\overline{\text{O}}$ H $\overline{\text{O}}$	0.8	10%	1.37	SSLB
	<i>tg</i> ⁺ 2 ₋₂	$\overline{\text{O}}$ $\overline{\text{O}}$ H	1.2	5.3%	1.43	SSLB
	<i>tg</i> ⁺ 3 ₋₂	$\overline{\text{O}}$ $\overline{\text{O}}$ H	1.5	3.1%	1.47	SSLB
	<i>g</i> ⁻ <i>g</i> ⁻ 1 ₋₂	$\overline{\text{H}}$ $\overline{\text{O}}$ $\overline{\text{O}}$	0.0	37%	1.47	SSLB
	<i>g</i> ⁻ <i>g</i> ⁻ 2 ₋₂	$\overline{\text{O}}$ $\overline{\text{O}}$ H	0.3	24%	1.46	SSLB
	<i>g</i> ⁻ <i>g</i> ⁻ 3 ₋₂	$\overline{\text{O}}$ H $\overline{\text{O}}$	0.9	8.2%	1.36	SSLB
	<i>g</i> ⁻ <i>g</i> ⁻ 4 ₋₂	$\overline{\text{H}}$ $\overline{\text{O}}$ $\overline{\text{O}}$	1.0	6.7%	1.44	SSLB
	<i>g</i> ⁻ <i>g</i> ⁻ 5 ₋₂	$\overline{\text{H}}$ $\overline{\text{O}}$ $\overline{\text{O}}$	1.3	4.0%	1.47	SSLB
-3	<i>tt</i> 1 ₋₃	$\overline{\text{O}}$ $\overline{\text{O}}$ $\overline{\text{O}}$	0.0	62%	–	–
	<i>tg</i> ⁺ 1 ₋₃	$\overline{\text{O}}$ $\overline{\text{O}}$ $\overline{\text{O}}$	0.4	33%	–	–
	<i>tg</i> ⁺ 2 ₋₃	$\overline{\text{O}}$ $\overline{\text{O}}$ $\overline{\text{O}}$	1.6	3.8%	–	–

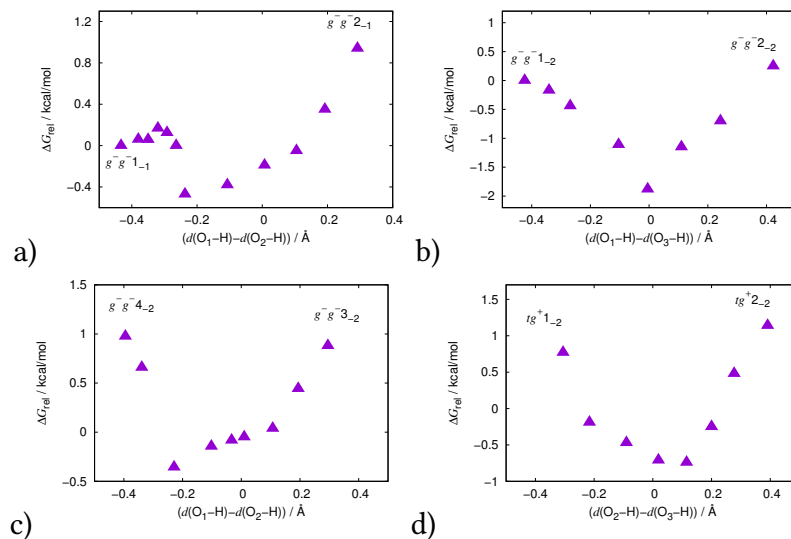


Figure 6: Free energy profiles for the intramolecular proton transfer between a) $g^-g^-1_{-1}$ and $g^-g^-1_{-1}$; b) $g^-g^-1_{-2}$ and $g^-g^-2_{-2}$; c) $g^-g^-3_{-2}$ and $g^-g^-4_{-2}$; d) tg^+1_{-2} and tg^+2_{-2} as a function of the deviation of the proton from its centered position in the hydrogen bond.

are obtained. The resulting macroscopic constants are in very good agreement with the values reported in previous literature using potentiometry. However, the found pair interaction energy between two terminal carboxylates and the triplet interaction energy are physically meaningless. The obtained interactions between two terminal charged groups are much larger than that between a terminal and the central groups. To be sure that this strange result is not an artifact produced by uncertainties in the fitting procedure, a robustness test based on random generation of synthetic data has been performed. Algebraic arguments also lead to the same conclusion.

This apparent contradiction suggested a more detailed analysis of the standard reaction scheme based on the SB model. As a consequence, full elucidation of the conformational structures for each ionization state of citric acid became necessary. Special attention has been paid for the formation of hydrogen bonds, due to their stabilizing effect. With this aim, *ab initio* MP2 calculations using the SMD polarizable continuum model for solvent were performed. When protons are constrained to be bound to a particular carboxylic group, the resulting micro-state probabilities are in reasonable agreement with the micro-speciation reported in previous works using selective blocking of the carboxylic groups. They were, however, in disagreement with the microstate

1
2
3
4 probabilities derived from the NMR titrations, specially in the case of the hydrogen-citrate ion.

5
6 A more careful analysis of the calculations suggested the possibility of proton delocaliza-
7
8 tion between two or even three carboxylate groups. The computations indicate that both di-
9
10 hydrogen and hydrogen citrate adopt stable conformations which could present proton delocal-
11
12 ization through low barrier HB between carboxyl groups. In the case of the hydrogen citrate ion,
13
14 we find that all the stable conformations (with probability near 100%) present this possibility. This
15
16 suggest a new reaction scheme including micro-species presenting delocalized proton binding.
17
18 In this new scheme, NMR would only detect a unique micro-species for the hydrogen-citrate ion.
19
20 This is what is concluded from the analysis of NMR titration data and would explain why when
21
22 the protons are constrained to be localized, the fundamental assumption of the SB model, non-
23
24 physical interaction energies are obtained. Micro-speciation of di-hydrogen citrate ion seems to
25
26 be better explained if delocalized proton binding is considered for some of the roto-microstates.

27
28 Delocalized proton binding in solution is an open and controversial issue, which has been
29
30 the subject of recent research. This work suggests that NMR in solution, combined with suitable
31
32 micro-speciation analysis and *ab initio* calculations, could shed some more light on this important
33
34 topic.
35
36
37

38 **Acknowledgement**

39
40 We acknowledge the financial support from Generalitat de Catalunya (Grants 2014SGR1017,
41
42 2014SGR1132 and XrQTC). J.L.G. acknowledge the Spanish Ministry of Science and Innovation
43
44 (project CTM2016-78798-C2-1-P). S.M., M.N. and F.M. acknowledge the funding of the 8SEWP -
45
46 HORIZON-2020 grant "Materials Networking" (692146).
47
48
49
50
51

52 **Supporting Information Available**

- 53
54
55 • An additional argument to the robustness of the found microscopic binding parameters.
56
57
58
59
60

- Additional figures showing free energy minimum conformations of citric acid obtained from *ab initio* optimizations in solvent for fully protonated, mono-deprotonated, di-deprotonated and fully deprotonated forms.
- Additional tables showing relative free energies and proportions of all conformations of citrate in water for charge states -1 and -2 obtained by MP2 calculations.

This material is available free of charge via the Internet at <http://pubs.acs.org/>.

References

- (1) Anastassiadis, S.; Morgunov, I.G.; Kamzolova, S.V.; Finogenova, T.V. Citric Acid Production Patent Review. *Recent Pat. Biotechnol.* **2008**, *2*, 107-123.
- (2) Pundir, R. K.; Jain, P. Evaluation of Five Chemical Food Preservatives for their Antibacterial Activity against Bacterial Isolates from Bakery Products and Mango Pickles. *J. Chem. Pharm. Res.* **2011**, *3*, 24-31.
- (3) Ling, C.; Liu, F.; Pei, Z.; Zhang, X.; Wei, M.; Zhang, Y.; Zheng, L.; Zhang, J.; Li, A.; Xing, B. Citric Acid Enhanced Copper Removal by a Novel Multi-amines Decorated Resin. *Sci. Rep.* **2015**, *5*, 9944.
- (4) Kimling, J.; Maier, M.; Okenve, B.; Kotaidis, V.; Ballot H.; Plech, A. Turkevich Method for Gold Nanoparticle Synthesis Revisited. *J. Phys. Chem. B* **2006**, *110*, 15700-15707.
- (5) Sasaki, S.; Kubota, N.; Doki, N. Adsorption Isotherms of Citric Acid Acting as a Growth-Suppressor onto the (100) and (111) Faces of Sodium Chloride Crystals in Supersaturated Aqueous Solution. *Chem. Eng. Technol.* **2006**, *29*, 247-250.
- (6) Bates, R. G.; Pinching, G. D. Resolution of the Dissociation Constants of Citric Acid at 0 to 50°, and Determination of Certain Related Thermodynamic Functions. *J. Am. Chem. Soc.* **1949**, *71*, 1274-1283.

- 1
2
3
4 (7) Bénézeth, P.; Palmer, D. A.; Wesolowski, D. J. Dissociation Quotients for Citric Acid in Aque-
5 ous Sodium Chloride Media to 150°C. *J. Solution Chem.* **1997**, *26*, 63-84.
6
7
8 (8) Crea, F.; De Stefano, C.; Millero, F. J.; Sharma, V. K. Dissociation Constants fo Citric Acid in
9 NaCl and KCl Solutions and their Mixtures at 25°C. *J. Solution Chem.* **2004**, *11*, 1349-1366.
10
11
12 (9) Kochergina, L. A.; Vasilev, V. P.; Krutov, D. V.; Krutova, O. N. A Thermochemical Study of
13 Acid-Base Interactions in Aqueous Solutions of Citric Acid. *Russian J. Phys. Chem.* **2007**, *81*,
14 182-186.
15
16
17
18
19 (10) Borkovec, M.; Koper, G. J. M. A Cluster Expansion Method for the Complete Resolution of
20 Microscopic Ionization Equilibria from NMR Titrations. *Anal. Chem.* **2000**, *72*, 3272-3279.
21
22
23 (11) Borkovec, M.; Jönsson, B.; Koper, G. J. M. In *Surface and Colloid Science*; Matijevic, E., Ed.;
24 Plenum Press: New York, 2001; Vol. 16. Ch. 2.
25
26
27
28 (12) Szakács, Z.; Kraszni, M.; Noszál, B. Determination of Microscopic Acid-Base Parameters
29 from NMR-pH Titrations. *Anal. Bioanal. Chem.* **2004**, *378*, 1428-1448.
30
31
32
33 (13) Loewenstein, A.; Roberts, J. D. The Ionization of Citric Acid Studied by the Nuclear Magnetic
34 Resonance Technique. *J. Am. Chem. Soc.* **1960**, *82*, 2705-2710.
35
36
37
38 (14) Martin, R. B. A Complete ionization Scheme for Citric Acid. *J. Phys. Chem.* **1961**, *65*,
39 2053-2055.
40
41
42
43 (15) Pearce, K. N.; Creamer, L. K. The Complete Ionization Scheme for Citric Acid. *Aust. J. Chem.*
44 **1975**, *28*, 2409-2415.
45
46
47
48 (16) Borkovec, M.; Hamacek, J.; Piguet, C. Statistical Mechanical Approach to Competitive Bind-
49 ing of Metal Ions to Multi-Center Receptors. *Dalton Trans.* **2004**, 4096-4105.
50
51
52
53 (17) Riss-Johannessen, T.; Favera, N. D.; Todorova, T. K.; Huber, S. M.; Gagliardi, L.; Piguet, C.
54 Understanding, Controlling and Programming Cooperativity in Self-Assembled Polynuclear
55 Complexes in Solution. *Chem. Eur. J.* **2009**, *15*, 12702-12718.
56
57
58
59
60

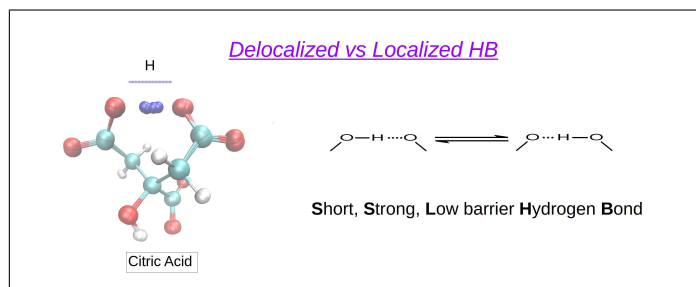
- 1
2
3
4 (18) Noszal, B.; Sandor, P. Rota-Microspeciation of Aspartic Acid and Asparagine. *Anal. Chem.*
5 **1989**, *61*, 2631-2637.
6
7
8
9 (19) Takeda, Y.; Samejima, K.; Nagano, K.; Watanabe, M.; Sugeta H.; Kyogoku, Y. Determination
10 of Protonation Sites in Thermospermine and in Some Other Polyamines by ^{15}N and ^{13}C
11 Nuclear Magnetic Resonance Spectroscopy. *Eur. J. Biochem.* **1983**, *130*, 383-389.
12
13
14
15 (20) Koper, G. J. M.; van Genderen, M. H. P.; Elissen-Román, C.; Baars, M. W. P. L.; Meijer, E.
16 J. ; Borkovec, M. Protonation Mechanism of Poly(propylene imine) Dendrimers and Some
17 Associated Oligo Amines. *J. Am. Chem. Soc.* **1997**, *119*, 6512-6521.
18
19
20
21
22 (21) Borkovec, M.; Spiess, B. Microscopic Ionization Mechanism of Inositol Tetrakisphosphates.
23 *Phys. Chem. Chem. Phys.* **2004**, *6*, 1144-1151.
24
25
26
27 (22) Riley, A. M.; Trusselle, M.; Kuad, P.; Borkovec, M.; Cho, J.; Choi, J. H.; Qian, X.; Shears,
28 S. B.; Spiess, B.; Potter, B. V. L. *scyllo*-Inositol Pentakisphosphate as an Analogue of *myo*-
29 Inositol 1,3,4,5,6-Pentakisphosphate: Chemical Synthesis, Physicochemistry and Biological
30 Applications. *ChemBioChem* **2006**, *7*, 1114-1122.
31
32
33
34
35
36 (23) Witanowski, M.; Stefaniak, L.; Webb, G. A. Nitrogen NMR Spectroscopy. *Annu. Rep. NMR*
37 *Spectrosc.* **1987**, *18*, 1-211.
38
39
40
41 (24) Moore, G. J.; Sillerud, L. O. The pH Dependence of Chemical Shift and Spin-Spin Coupling
42 for Citrate. *J. Magnetic Resonance Series B* **1994**, *103*, 87-88.
43
44
45
46 (25) Cleland, W. W. The Low-Barrier Hydrogen Bond in Enzymatic Catalysis. *Adv. Phys. Org.*
47 *Chem.* **2010**, *44*, 1-17.
48
49
50
51 (26) Ellison, R. D.; Levy, H. A. A Centered Hydrogen Bond in Potassium Hydrogen Chloroma-
52 leate: A Neutron Diffraction Structure Determination. *Acta Cryst.* **1965**, *19*, 260-268.
53
54
55
56 (27) Steiner, T.; Majerz, I.; Wilson, C. C. First O-H-N Hydrogen Bond with a Centered Proton
57 Obtained by Thermally Induced Proton Migration. *Angew. Chem.* **2001**, *40*, 2651-2654.
58
59
60

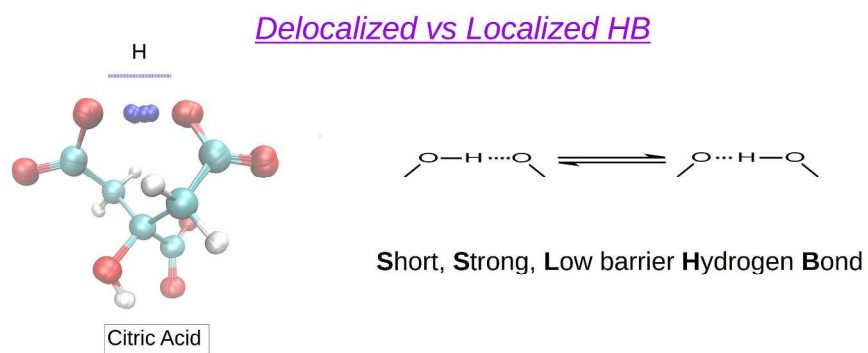
- 1
2
3
4 (28) Perrin, C. L. Are Short, Low-Barrier Hydrogen Bonds Unusually Strong? *Acc. Chem.*
5 *Res.* **2010**, *43*, 1550-1557.
6
7
8
9 (29) Stasko, D.; Hoffmann, S. P.; Kim, K.-C.; Fackler, N. L. P.; Larsen, A. S.; Drovetskaya, T.; Tham,
10 F. S.; Reed, C. A.; Richard, C. E. F.; Boyd, P. D. W.; Stoyanov, E. S. Molecular Structure of the
11 Solvated Proton in Isolated Salts. Short, Strong, Low Barrier (SSLB) H-bonds. *J. Am. Chem.*
12 *Soc.* **2002**, *124*, 13869-13876.
13
14
15
16
17 (30) Reed, C. A. Myths about the Proton. The Nature of H⁺ in Condensed Media. *Acc. Chem. Res.*
18 **2013**, *46*, 2567-2575.
19
20
21
22 (31) Kawaguchi, S.; Kitano, T.; Ito, K. Dissociation Behaviour of Poly(fumaric acid) and
23 Poly(maleic acid). 3. Infrared and Ultraviolet Spectroscopy. *Macromolecules* **1992**, *25*, 1294-
24 1299.
25
26
27
28
29 (32) Kolesnikov, S. P.; Lyudkovskaya, I. V.; Antipin, M. Yu.; Struchnov, T. Yu.; Neferov, O. M.
30 Etherates of Friedel-Crafts Acids with a Short Hydrogen Bond: Symmetrical [Et₂O.....OEt₂]⁺
31 Cation in the Crystal Structure of the Etherate (Et₂O)₂·ZnCl₃. *Bull. Acad. Sci. USSR,*
32 *Chem. Sci.* **1985**, *34*, 74-80.
33
34
35
36
37
38 (33) Perrin, C. L. Symmetries of Hydrogen Bonds in Solution. *Science*, **1994**, *266*, 1665-1668.
39
40
41 (34) Garcia-Viloca, M.; González-Lafont, A.; Lluch, J. M. Asymmetry of the Hydrogen Bond of
42 Hydrogen Phthalate Anion in Solution. A QM/MM Study. *J. Am. Chem. Soc.* **1999**, *121*, 9198-
43 9207.
44
45
46
47
48 (35) Khan, M. A. S.; Sen, A.; Ganguly, B. Probing the Influence of pH Dependent Citric Acid
49 Towards the Morphology of Rock Salt: a Computational Study. *CrystEngComm* **2009**, *11*,
50 2660-2667.
51
52
53
54
55 (36) Wright, L. B.; Rodger, P. M.; Walsh, T. R. Aqueous Citrate: a First-Principles and Force-Field
56 Molecular Dynamics Study. *RCS Adv.* **2013**, *3*, 16399-16409.
57
58
59
60

- 1
2
3
4 (37) Marenich, A. V.; Cramer, C. J.; Truhlar, D. G. Universal Solvation Model Based on Solute
5 Electron Density and on a Continuum Model of the Solvent Defined by the Bulk Dielectric
6 Constant and Atomic Surface Tensions. *J. Phys. Chem. B* **2009**, *113*, 6378-6396.
7
8
9
10 (38) Garcés, J. L.; Koper, G. J. M.; Borkovec, M. Ionization Equilibria and Conformational Transi-
11 tions in Polyprotic Molecules and Polyelectrolytes. *J. Phys. Chem. B* **2006**, *110*, 10937-10950.
12
13
14
15 (39) Garcés, J. L.; Madurga, S.; Borkovec, M. Coupling of Conformational and Ionization Equi-
16 libria in Linear Poly(ethylenimine): a Study Based on the Site Binding/Rotational Isomeric
17 State (SBRIS) Model. *Phys. Chem. Chem. Phys.* **2014**, *16* 4626-4638.
18
19
20
21
22 (40) Slichter, C. P. *Principles of Magnetic Resonance*. Springer. Berlin, 1980.
23
24
25 (41) Flory, P. L. *Statistical Mechanics of Chain Molecules*; John Wiley: New York, 1969.
26
27
28 (42) Frisch, M. J.; Trucks, G. W.; Schlegel, H. B.; Scuseria, G. E.; Robb, M. A.; Cheeseman, J. R.;
29 Scalmani, G.; Barone, V.; Mennucci, B.; Petersson, G. A.; Gaussian 09, revision D01, 2012;
30 Gaussian, Inc.: Wallingford, CT, 2009.
31
32
33
34 (43) Kolar, M.; Fanfrlik, J.; Lepsik, M.; Forti, F.; Luque, F. J.; Hobza, P. Assessing the Accuracy
35 and Performance of Implicit Solvent Models for Drug Molecules: Conformational Ensemble
36 Approaches. *J. Phys. Chem. B* **2013**, *117*, 5950-5962.
37
38
39
40
41
42 (44) French, A. D.; Johnson, G. P.; Cramer, C. J.; Csonka, G. I. Conformational Analysis of Cel-
43 lobiose by Electronic Structure Theories. *Carbohydrate Research* **2012**, *350*, 68-76.
44
45
46
47 (45) Yao, G.; Zhang, J.; Huang, Q. Conformational and Vibrational Analyses of Meta-Tyrosine:
48 an Experimental and Theoretical Study. *Spectrochim. Acta Mol. Biomol. Spectrosc.* **2015**, *151*,
49 111-123.
50
51
52
53
54 (46) Ribeiro, R. F.; Marenich, A. V.; Cramer, C. J.; Truhlar, D. G. Use of Solution-Phase Vibrational
55 Frequencies in Continuum Models for the Free Energy of Solvation. *J. Phys. Chem B* **2011**,
56 *115*, 14556-14562.
57
58
59
60

- 1
2
3
4 (47) MATLAB version 7.10.0. Natick, Massachusetts: The MathWorks Inc., 2010.
5
6
7 (48) Alper, J. S.; Gelb, R. I. Standard Errors and Confidence Intervals in Nonlinear Regression:
8 Comparison of Monte Carlo and Parametric Statistics. *J. Phys. Chem.* **1990**, *94*, 4747-4751.
9
10
11 (49) Press, W. H.; Teukolsky, S. A.; Vetterling, W. T.; Flannery B. P. *Numerical Recipes in Fortran*
12 *77: the art of scientific computing* 1986-1992. Cambridge University Press. *Ch. 15*.
13
14
15
16 (50) De Robertis, A.; De Stefano, C.; Rigano, C.; Sammartano, S. Thermodynamic Parameters for
17 the Protonation of Carboxylic Acids in Aqueous Tetraethylammonium Iodide Solutions. *J.*
18 *Solution Chem.* **1990**, *19*, 569-587.
19
20
21
22
23 (51) de Groot, J.; Koper, G. J. M.; Borkovec, M.; de Bleijser, J. Dissociation Behavior of Poly(maleic
24 acid): Potentiometric Titrations, Viscometry, Pulsed Field Gradient NMR, and Model Calculations.
25 *Macromolecules* **1998**, *31*, 4182-4188.
26
27
28
29
30 (52) Smits, R. G.; Koper, G. J. M.; Mandel, M. The Influence of Nearest- and Next-Nearest-
31 Neighbor Interactions on the Potentiometric Titration of Linear Poly(ethylenimine). *J. Phys.*
32 *Chem.* **1993**, *97*, 5745-5751.
33
34
35
36
37 (53) Lugo, M. L.; Lubes, V. R. Ternary Complex Formation between Chromium(III)-Picolinic Acid,
38 Chromium(III)-Dipicolinic Acid, and Small Blood Serum Biologands. *J. Chem. Eng. Data* **2007**,
39 *52*, 1217-1222.
40
41
42
43
44 (54) Wyrzykowski, D.; Czupryniak, J.; Ossowski, T.; Chmurzynski, L. Thermodynamic Interac-
45 tions of the Alkaline Earth Metal Ions with Citric Acid. *J. Therm. Anal. Calorim.* **2010**, *102*,
46 149-154.
47
48
49
50
51 (55) Camoes, M. F.; Lito, M. J. G.; Ferra, M. I. A.; Covington, A. K. Consistency of pH Standard
52 Values with the Corresponding Thermodynamic Acid Dissociation Constants. *Pure&Appl.*
53 *Chem.* **1997**, *69*, 1325-1333.
54
55
56
57
58 (56) Schreckenbach, G. Differential Solvation. *Chem. Eur. J.* **2017**, *23*, 3797-3803.
59
60

Graphical TOC Entry





Delocalized Proton Binding of Citric Acid

900x350mm (96 x 96 DPI)

Supporting Information

Ionization and Conformational Equilibria of Citric Acid: Delocalized Proton Binding in Solution

Sergio Madurga^{a*}, Miroslava Nedyalkova^b, Francesc Mas^a and Josep Lluís Garcés^c

^a Materials Science and Physical Chemistry Department & Research Institute of Theoretical and Computational Chemistry (IQTUB) of Barcelona University (UB), C/ Martí i Franquès, 1. 08028 Barcelona (Catalonia, Spain)

^b Inorganic Chemistry Department, Faculty of Chemistry and Pharmacy “St Kliment Ohridski”, University of Sofia, 1 James Bourchier Blvd. 1164, Sofia (Bulgaria)

^c Chemistry Department and AGROTECNIO, University of Lleida (UdL), Rovira Roure, 191, 25198, Lleida (Catalonia, Spain)

* corresponding author. e-mail: s.madurga@ub.edu; www.ub.edu/biophyschem

The reported best-fitted parameters correspond to the unique local minimum of the fitting procedure. An additional argument to the robustness of the found microscopic binding parameters.

Let us outline an argument to show that the best-fitted parameters shown in this work correspond to a unique minimum of the fitting process. Firstly note that by rewriting the equations

$$\begin{aligned}\delta &= \delta_0 + \delta_{13}\theta_1 + (\delta_P - \delta_0 - \delta_{13})\theta_2 \\ \Delta &= \Delta_0 + \Delta_{13}\theta_1 + (\Delta_P - \Delta_0 - \Delta_{13})\theta_2\end{aligned}\quad (1)$$

replacing

$$\begin{cases} \theta_1(a_H) = \pi_1(\text{H}\Theta\Theta)P_1(a_H) + (1 - \pi_2(\text{H}\text{H}\Theta))P_2(a_H) + P_3(a_H) \\ \theta_2(a_H) = (1 - 2\pi_1(\text{H}\Theta\Theta))P_1(a_H) + 2\pi_2(\text{H}\text{H}\Theta)P_2(a_H) + P_3(a_H) \end{cases}\quad (2)$$

in eqn. (1), δ and Δ can be expressed in terms of the macroscopic probabilities $P_i(a_H)$, which only depend on the macroscopic dissociation pK_i -values *via*

$$P_n(a_H) = \frac{\overline{K}_n a_H^n}{\Xi}; \quad \Xi = \sum_{i=0, \dots, N} \overline{K}_i a_H^i; \quad pK_i = -\log K_i = \log(\overline{K}_{N-i+1}/\overline{K}_{N-i})\quad (3)$$

Introducing Eqns. (2) in (1) we obtain δ and Δ as a linear combination of the macroscopic probabilities. As a result we obtain the equations

$$\begin{aligned}\delta &= \delta_0 + X P_1(a_H) + Y P_2(a_H) + (\delta_P - \delta_0) P_3(a_H) \\ \Delta &= \Delta_0 + x P_1(a_H) + y P_2(a_H) + (\Delta_P - \Delta_0) P_3(a_H)\end{aligned}\quad (4)$$

where X , Y , x and y are new parameters to be fitted and defined as

$$\begin{aligned} X &= (2\delta_0 - 2\delta_P + 3\delta_{13}) \pi_1(\text{H}\Theta\Theta) + (\delta_P - \delta_0 - \delta_{13}) \\ Y &= (2\delta_P - 2\delta_0 - 3\delta_{13}) \pi_2(\text{H}\text{H}\Theta) + \delta_{13} \\ x &= (2\Delta_0 - 2\Delta_P + 3\Delta_{13}) \pi_1(\text{H}\Theta\Theta) + (\Delta_P - \Delta_0 - \Delta_{13}) \\ y &= (2\Delta_P - 2\Delta_0 - 3\Delta_{13}) \pi_2(\text{H}\text{H}\Theta) + \Delta_{13} \end{aligned} \quad (5)$$

But we have very good values for the macroscopic dissociation constants, obtained previously by potentiometry. Recalling too that δ_P , δ_0 , Δ_P and Δ_0 do not need to be fitted (they are directly obtained from the chemical shifts at very low and very high pH-values), we get that Eqns. (4) reduce to a *linear* fitting of X , Y , x and y . As a result, only *one minimum* can be obtained in fitting eqn. (4) to the experimental NMR curves. Thus, the values of X , Y , x and y are uniquely determined. The obtained values are (within the experimental and numerical error) $X=0.137$, $Y=0.266$, $x=-15.14$, $y=-5.65$.

With those values for X , Y , x and y at hand, the problem reduces to show that the solution of the system of Eqns. (5), containing four unknowns ($\pi_1(\text{H}\Theta\Theta)$, $\pi_2(\text{H}\text{H}\Theta)$, δ_{13} and Δ_{13}) is unique for values of $\pi_1(\text{H}\Theta\Theta)$ and $\pi_2(\text{H}\text{H}\Theta)$ lying between 0 and 1. This is an elementary exercise of algebra and numerical computation by eliminating δ_{13} and Δ_{13} from the system of equations and analysing the solutions for the resulting 2-equations system for $\pi_1(\text{H}\Theta\Theta)$ and $\pi_2(\text{H}\text{H}\Theta)$. It is found that the only solution (within the experimental and numerical error) corresponds to

$$\pi_1(\text{H}\Theta\Theta) \simeq 0.5; \pi_2(\text{H}\text{H}\Theta) \simeq 0.20 \quad (6)$$

which are very close to the obtained values by direct fitting of all the microscopic binding parameters to the experimental NMR shift data. Furthermore, recalling that

$$\pi_2(\text{H}\text{H}\Theta) = \frac{1}{2 + \frac{k_2}{k_1}} \simeq 0.20 \Rightarrow k_2/k_1 \simeq 3 \quad (7)$$

which is very close to the ratio obtained by direct fitting. Replacing (7) in the expression for $\pi_1(\text{H}\Theta\Theta)$

$$\pi_1(\text{H}\Theta\Theta) = \frac{1}{2 + \frac{k_1 v}{k_2 u}} \simeq 0.5 \Rightarrow \frac{v}{3u} \simeq 0 \quad (8)$$

so that the repulsive interaction between terminal charged groups must be larger than the interaction terminal-central group.

FIGURES of Supplementary Information

Free energy minimum conformations of citric acid obtained from *ab initio* optimizations in solvent for fully protonated (Fig. S1), mono-deprotonated (Fig. S2), di-deprotonated (Fig. S3) and fully deprotonated (Fig S4) forms. In Fig S2 and S3, it is also indicated the labelling to specify the state of each of the three carboxylic groups: “H” specifies a protonated carboxylic group and “ \ominus ” specifies a deprotonated carboxylic group. The participation of a carboxylic group in a intramolecular hydrogen bond is indicated by a overbar over the corresponding “H” or “ \ominus ” site.

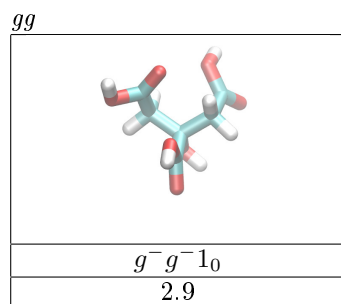
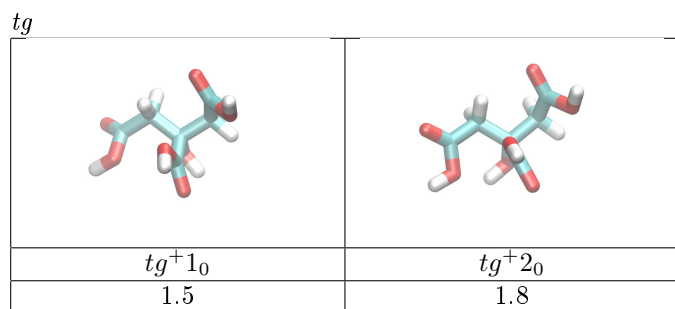
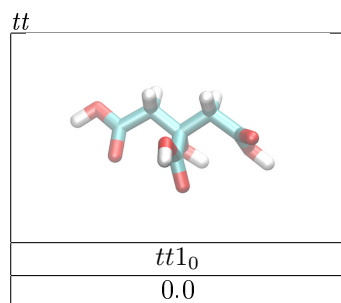


Figure S1: *tt*, *tg* and *gg* minimum conformations of citric acid obtained from optimizations at MP2 level with the SMD water model with the 6-311++G(d,p) basis set for charge state 0. The labeling indicates the conformation of each of the two principal dihedral angles (*t* for *trans*, *g* for *gauche*). The (+,-) superscript of *g* indicates the sign of the *gauche* angle. Relative free energies with respect to the most stable minimum conformation for each charge state in kcal/mol. The color of atoms correspond to blue for carbon, red for oxygen, white for hydrogen. Intermolecular hydrogen bonds are also indicated by red dashed lines.

tt

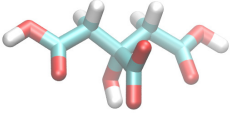
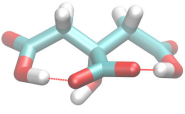
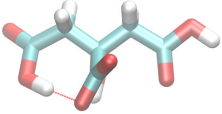
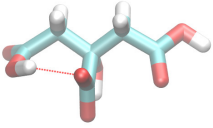
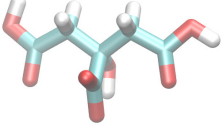
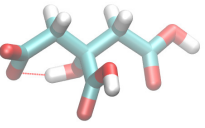
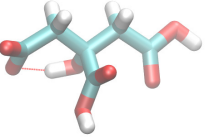
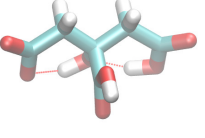
		
<i>tt1</i> ₋₁ HΘH	<i>tt2</i> ₋₁ HΘH	<i>tt3</i> ₋₁ HΘH
0	1.5	1.6
		
<i>tt4</i> ₋₁ HΘH	<i>tt5</i> ₋₁ HΘH	<i>tt6</i> ₋₁ ΘHH
2.1	2.2	2.5
		
<i>tt7</i> ₋₁ ΘHH	<i>tt8</i> ₋₁ ΘHH	
2.6	2.7	

Figure S2: *tt* minimum conformations of citric acid obtained from optimizations at MP2 level with the SMD water model with the 6-311++G(d,p) basis set for charge state -1. The same preferences and units as indicated in Fig S1 were used.

tg

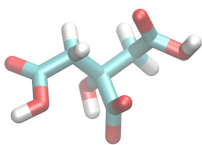
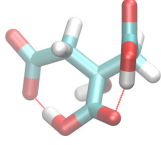
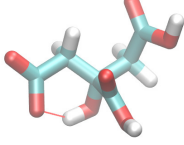
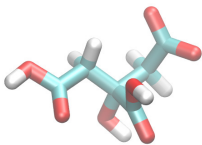
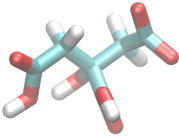
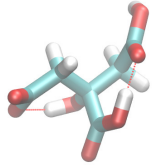
		
$tg^{+1-1} \text{H}\Theta\text{H}$ 1.2	$tg^{+2-1} \overline{\Theta}\text{H}\overline{\text{H}}$ 3.2	$tg^{+3-1} \overline{\Theta}\text{H}\overline{\text{H}}$ 3.7
		
$tg^{+4-1} \text{H}\text{H}\Theta$ 4.9	$tg^{+5-1} \text{H}\text{H}\Theta$ 6.8	$tg^{+6-1} \overline{\Theta}\text{H}\overline{\text{H}}$ 7.0

Figure S3: *tg* minimum conformations of citric acid obtained from optimizations at MP2 level with the SMD water model with the 6-311++G(d,p) basis set for charge state -1. The same preferences and units as indicated in Fig S1 were used.

Fig. S3. Minimum conformations of citric acid obtained from optimizations at MP2 level with the SMD water model with the 6-311++G(d,p) basis set for charge state -2. The same preferences and units as indicated in Fig S1 were used.

gg

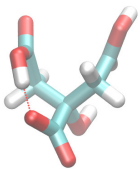
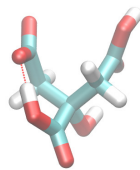
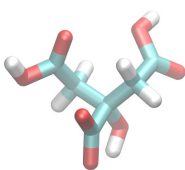
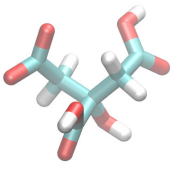
		
$g^-g^-1_{-1} \text{H}\Theta\text{H}$ 0.0	$g^-g^-2_{-1} \Theta\text{H}\text{H}$ 0.9	$g^-g^-3_{-1} \text{H}\Theta\text{H}$ 2.6
		
$g^-g^-4_{-1} \Theta\text{H}\text{H}$ 8.4		

Figure S4: *gg* minimum conformations of citric acid obtained from optimizations at MP2 level with the SMD water model with the 6-311++G(d,p) basis set for charge state -1. The same preferences and units as indicated in Fig S1 were used.

tt

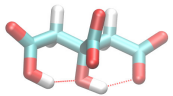
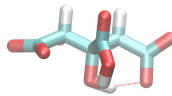
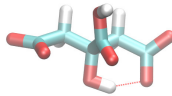
		
$tt1_{-2} \text{H}\Theta\Theta$ 3.4	$tt2_{-2} \Theta\text{H}\Theta$ 3.9	$tt3_{-2} \Theta\text{H}\Theta$ 4.8

Figure S5: *tt* minimum conformations of citric acid obtained from optimizations at MP2 level with the SMD water model with the 6-311++G(d,p) basis set for charge state -2. The same preferences and units as indicated in Fig S1 were used.

tg

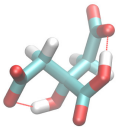
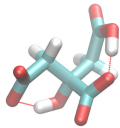
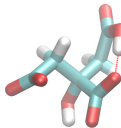
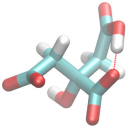
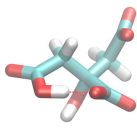
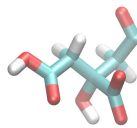
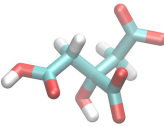
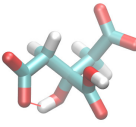
		
$tg^{+1-2} \Theta H \bar{\Theta}$ 0.8	$tg^{+2-2} \Theta \bar{H} \bar{H}$ 1.2	$tg^{+3-2} \Theta \bar{H} \bar{H}$ 1.5
		
$tg^{+4-2} \Theta \bar{H} \bar{H}$ 3.5	$tg^{+5-2} \bar{H} \bar{H} \bar{\Theta}$ 5.0	$tg^{+6-2} H \bar{\Theta} \bar{\Theta}$ 5.0
		
$tg^{+7-2} H \bar{\Theta} \bar{\Theta}$ 5.1	$tg^{+8-2} \Theta H \bar{\Theta}$ 6.1	

Figure S6: *tg* minimum conformations of citric acid obtained from optimizations at MP2 level with the SMD water model with the 6-311++G(d,p) basis set for charge state -2. The same preferences and units as indicated in Fig S1 were used.

gg

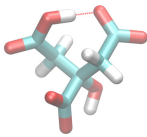
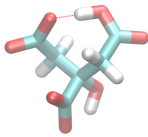
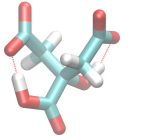
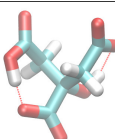
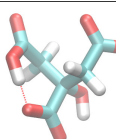
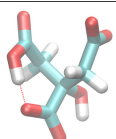
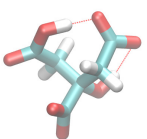
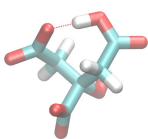
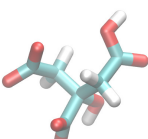
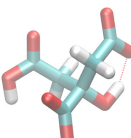
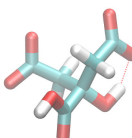
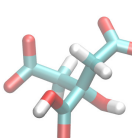
		
$g^-g^-1_{-2} \bar{H}\bar{\Theta}\bar{\Theta}$ 0.0	$g^-g^-2_{-2} \bar{\Theta}\bar{\Theta}H$ 0.3	$g^-g^-3_{-2} \bar{\Theta}H\bar{\Theta}$ 0.9
		
$g^-g^-4_{-2} \bar{H}\bar{\Theta}\bar{\Theta}$ 1.0	$g^-g^-5_{-2} \bar{H}\bar{\Theta}\bar{\Theta}$ 1.3	$g^-g^-6_{-2} \bar{H}\bar{\Theta}\bar{\Theta}$ 2.8
		
$g^-g^-7_{-2} \bar{H}\bar{\Theta}\bar{\Theta}$ 3.0	$g^-g^-8_{-2} \bar{\Theta}\bar{\Theta}H$ 3.3	$g^-g^-9_{-2} \bar{\Theta}\bar{\Theta}H$ 6.7
		
$g^-g^-10_{-2} H\bar{\Theta}\bar{\Theta}$ 7.6	$g^-g^-11_{-2} \bar{\Theta}H\bar{\Theta}$ 7.7	$g^-g^-12_{-2} \bar{\Theta}H\bar{\Theta}$ 11.1

Figure S7: *gg* minimum conformations of citric acid obtained from optimizations at MP2 level with the SMD water model with the 6-311++G(d,p) basis set for charge state -2. The same preferences and units as indicated in Fig S1 were used.

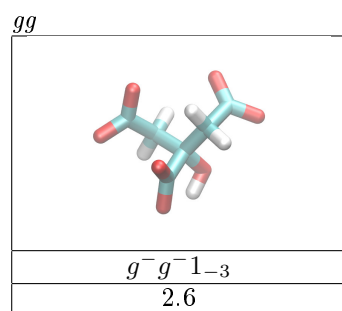
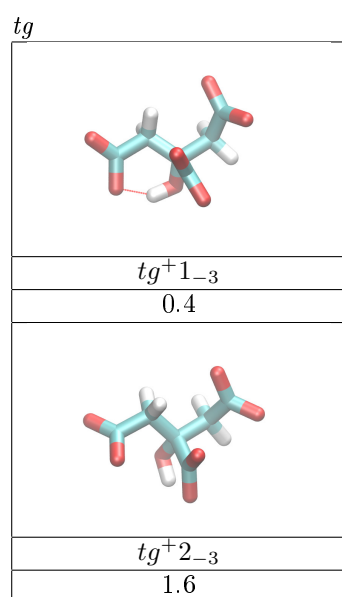
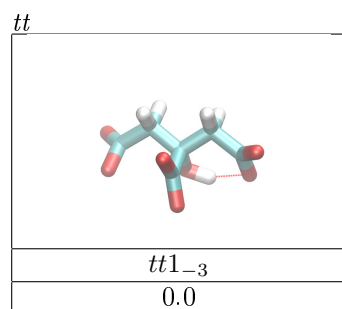


Figure S8: *tt*, *tg* and *gg* Minimum conformations of citric acid obtained from optimizations at MP2 level with the SMD water model with the 6-311++G(d,p) basis set for charge state -3. The same preferences and units as indicated in Fig S1 were used.

TABLES of Supplementary Information

Tables S1 and S2 show relative free energies and proportions of all conformations of citrate in water for charge states -1 and -2 obtained by MP2 calculations.

Table S1: Relative Free energies (in kcal/mol) in water of different conformations for the mono-deprotonated form of citrate. Conformational proportions are calculated at 25°C. “H” specifies a protonated carboxylic group and “Θ” specifies a deprotonated carboxylic group. The participation of a carboxylic group in a intramolecular hydrogen bond between two carboxylic groups is indicated by an overbar over the corresponding “H” or “Θ” site.

conformation		ΔG_{rel}	Relative population
$tt1_{-1}$	HΘH	0	23%
$tt2_{-1}$	$\overline{\text{H}\Theta\text{H}}$	1.5	3.7%
$tt3_{-1}$	$\overline{\text{H}\Theta\text{H}}$	1.6	3.2%
$tt4_{-1}$	$\overline{\text{H}\Theta\text{H}}$	2.1	1.5%
$tt5_{-1}$	HΘH	2.2	1.1%
$tt6_{-1}$	ΘHH	2.5	0.8%
$tt7_{-1}$	ΘHH	2.6	0.6%
$tt8_{-1}$	ΘHH	2.7	0.5%
tg^+1_{-1}	HΘH	1.2	6.1%
tg^+2_{-1}	$\overline{\Theta\text{H}\text{H}}$	3.2	0.2%
tg^+3_{-1}	ΘHH	3.7	0.1%
tg^+4_{-1}	HHΘ	4.9	0.0%
tg^+5_{-1}	HHΘ	6.8	0.0%
tg^+6_{-1}	$\overline{\Theta\text{H}\text{H}}$	7.0	0.0%
$g^-g^-1_{-1}$	$\overline{\text{H}\Theta\text{H}}$	0.0	48%
$g^-g^-2_{-1}$	$\overline{\Theta\text{H}\text{H}}$	0.9	10%
$g^-g^-3_{-1}$	HΘH	2.6	0.6%
$g^-g^-4_{-1}$	ΘHH	8.4	0.0%

Table S2: Relative Free energies (in kcal/mol) in water of different conformations for the di-deprotonated form of citrate. Conformational proportions are calculated at 25°C. Charged carboxylic groups and intramolecular hydrogen bonds are indicated as in Table S1.

conformation		$\Delta G_{rel}^{\ddagger}$	Relative population
$tt1_{-2}$	H $\Theta\Theta$	3.4	0.1%
$tt2_{-2}$	$\Theta H\Theta$	3.9	0.1%
$tt3_{-2}$	$\Theta H\bar{\Theta}$	4.8	0.0%
tg^+1_{-2}	$\Theta H\bar{\Theta}$	0.8	10%
tg^+2_{-2}	$\Theta\Theta\bar{H}$	1.2	5.3%
tg^+3_{-2}	$\Theta\Theta\bar{H}$	1.5	3.1%
tg^+4_{-2}	$\Theta\Theta\bar{H}$	3.5	0.1%
tg^+5_{-2}	$\bar{H}\Theta\Theta$	5.0	0.0%
tg^+6_{-2}	H $\Theta\Theta$	5.0	0.0%
tg^+7_{-2}	H $\Theta\Theta$	5.1	0.0%
tg^+8_{-2}	$\Theta H\Theta$	6.1	0.0%
$g^-g^-1_{-2}$	$\bar{H}\Theta\bar{\Theta}$	0.0	37%
$g^-g^-2_{-2}$	$\bar{\Theta}\Theta\bar{H}$	0.3	24%
$g^-g^-3_{-2}$	$\bar{\Theta}\bar{H}\Theta$	0.9	8.3%
$g^-g^-4_{-2}$	$\bar{H}\bar{\Theta}\Theta$	1.0	6.8%
$g^-g^-5_{-2}$	$\bar{H}\bar{\Theta}\Theta$	1.3	4.0%
$g^-g^-6_{-2}$	$\bar{H}\bar{\Theta}\Theta$	2.8	0.3%
$g^-g^-7_{-2}$	$\bar{H}\Theta\bar{\Theta}$	3.0	0.3%
$g^-g^-8_{-2}$	$\bar{\Theta}\Theta\bar{H}$	3.3	0.1%
$g^-g^-9_{-2}$	$\Theta\Theta H$	6.7	0.0%
$g^-g^-10_{-2}$	H $\Theta\Theta$	7.6	0.0%
$g^-g^-11_{-2}$	$\Theta H\Theta$	7.7	0.0%
$g^-g^-12_{-2}$	$\Theta H\Theta$	11.1	0.0%